

RESEARCH

Open Access



Neutrophil-specific expression of JAK2-V617F or CALRmut induces distinct inflammatory profiles in myeloproliferative neoplasia

Tobias Ronny Haage^{1,2†}, Emmanouil Charakopoulos^{1,2†}, Vikas Bhuria^{2,3,5}, Conny K. Baldauf³, Mark Korthals^{2,4}, Juliane Handschuh^{2,3}, Peter Müller^{1,2}, Juan Li⁶, Kunjan Harit⁷, Gopala Nishanth⁷, Stephanie Frey^{1,2}, Martin Böttcher^{1,2}, Klaus-Dieter Fischer^{2,4}, Jan Dudeck^{2,3}, Anne Dudeck^{2,3}, Daniel B. Lipka^{8,9}, Burkhardt Schraven^{2,3,5}, Anthony R. Green⁶, Andreas J. Müller^{2,3,5,10}, Dimitrios Mougiakakos^{1,2} and Thomas Fischer^{2,3,5*}

Abstract

Background Neutrophils play a crucial role in inflammation and in the increased thrombotic risk in myeloproliferative neoplasms (MPNs). We have investigated how neutrophil-specific expression of JAK2-V617F or CALRdel re-programs the functions of neutrophils.

Methods Ly6G-Cre JAK2-V617F and Ly6G-Cre CALRdel mice were generated. MPN parameters as blood counts, splenomegaly and bone marrow histology were compared to wild-type mice. Megakaryocyte differentiation was investigated using lineage-negative bone marrow cells upon in vitro incubation with TPO/IL-1 β . Cytokine concentrations in serum of mice were determined by Mouse Cytokine Array. IL-1 α expression in various hematopoietic cell populations was determined by intracellular FACS analysis. RNA-seq to analyse gene expression of inflammatory cytokines was performed in isolated neutrophils from JAK2-V617F and CALR-mutated mice and patients. Bioenergetics of neutrophils were recorded on a Seahorse extracellular flux analyzer. Cell motility of neutrophils was monitored in vitro (time lapse microscopy), and in vivo (two-photon microscopy) upon creating an inflammatory environment. Cell adhesion to integrins, E-selectin and P-selection was investigated in-vitro. Statistical analysis was carried out using GraphPad Prism. Data are shown as mean \pm SEM. Unpaired, two-tailed t-tests were applied.

Results Strikingly, neutrophil-specific expression of JAK2-V617F, but not CALRdel, was sufficient to induce pro-inflammatory cytokines including IL-1 in serum of mice. RNA-seq analysis in neutrophils from JAK2-V617F mice and patients revealed a distinct inflammatory chemokine signature which was not expressed in CALR-mutant neutrophils. In addition, IL-1 response genes were significantly enriched in neutrophils of JAK2-V617F patients as compared to CALR-mutant patients. Thus, JAK2-V617F positive neutrophils, but not CALR-mutant neutrophils, are pathogenic

[†]Tobias Ronny Haage and Emmanouil Charakopoulos contributed equally to this work.

*Correspondence:
Thomas Fischer
thomas.fischer@med.ovgu.de

Full list of author information is available at the end of the article



drivers of inflammation in MPN. In line with this, expression of JAK2-V617F or CALRdel elicited a significant difference in the metabolic phenotype of neutrophils, suggesting a stronger inflammatory activity of JAK2-V617F cells. Furthermore, JAK2-V617F, but not CALRdel, induced a VLA4 integrin-mediated adhesive phenotype in neutrophils. This resulted in reduced neutrophil migration *in vitro* and in an inflamed vessel. This mechanism may contribute to the increased thrombotic risk of JAK2-V617F patients compared to CALR-mutant individuals.

Conclusions Taken together, our findings highlight genotype-specific differences in MPN-neutrophils that have implications for the differential pathophysiology of JAK2-V617F versus CALR-mutant disease.

Keywords MPN, Inflammation, Neutrophils, JAK2-V617F, CALR mutations

Background

The discovery of JAK2-V617F, an activating somatic gain-of-function mutation of the Janus kinase 2 (JAK2), in classic Philadelphia chromosome-negative chronic myeloproliferative neoplasms (MPNs) such as essential thrombocythemia (ET), polycythemia vera (PV), and primary myelofibrosis (PMF), has provided first insight into the molecular basis of MPN. Genomic analysis revealed the occurrence of JAK2-V617F in the majority (95%) of PV patients and in 50% of ET and PMF patients [1–3]. Somatic mutations within the Calreticulin (*CALR*) gene, a major endoplasmic reticulum (ER) chaperone, are detected in 60–80% of JAK2 and thrombopoietin receptor (MPL) non-mutated ET and PMF patients [4, 5]. Calreticulin mutations are located in exon 9 and are classified as either type 1 mutation, exemplified by a 52 bp deletion, or type 2 mutation, exemplified by a 5 bp insertion [5]. All *CALR* mutations generate a novel C-terminus in the mutant protein [6]. Notably, in hematopoietic cells, *CALR* mutations (*CALRmut*) have been associated with an indirect activation of the JAK2-STAT pathway via MPL, accomplished through binding of mutated *CALR* to its extracellular domain [7–9]. However, due to *CALR*'s chaperone functions in the ER, *CALRmut* also activates additional signaling pathways. These include the activation of the unfolded protein response [10–12], defective interaction of *CALRmut* with the store-operated calcium entry (SOCE) machinery [13] and modulation of binding to known and as yet unidentified partners [14]. JAK2-V617F and *CALRmut* are the most frequent genetic alterations in MPNs and are responsible for driving the pathophysiology of the disease [1, 5, 15]. The genetic signature predicts clinical phenotypes such as abnormal blood counts, risk of leukemic transformation and event-free survival [16].

A key characteristic of JAK2- and *CALR*-mutated MPN is a chronic non-resolving inflammatory condition that promotes clonal evolution [17–20]. Importantly, recent research has revealed that chronic inflammation in MPN is indeed a driver of leukemic transformation [21]. In addition, a major cause of morbidity and mortality in MPN is venous and arterial thrombosis. In PV, large clinical studies revealed an incidence of 20–23% thrombotic

events at diagnosis [22–24]. However, according to a recent meta-analysis in PMF, *CALR*-mutated patients demonstrated a lower risk of thrombosis than JAK2-mutated patients [25]. In myelofibrosis, *CALR*-mutated patients also displayed a distinct disease phenotype compared to JAK2-V617F positive individuals: *CALR* mutated patients presented with less frequent inflammatory symptoms upon diagnosis, fewer thrombotic complications and less prominent splenomegaly [26]. A similar genotype-phenotype correlation is evident in ET: *CALR* mutated individuals are substantially different from JAK2-V617F positive patients in terms of hematologic and clinical features [27]. Furthermore, despite having lower platelet (PLT) counts, JAK2-V617F positive ET patients have twice the risk of thrombotic complications compared to those with *CALR* mutations [27]. This paradoxical observation suggests that JAK2-V617F induced alterations in adhesion properties of granulocytes, erythrocytes, PLTs and endothelial cells might be more relevant to the pathogenesis of thrombosis than the PLT counts *per se* [28–30]. This view is supported by research on clinical samples, which revealed high neutrophil-PLT aggregates in ET and PV patients, as well as increased activation of PLTs, leukocytes, and coagulation in MPNs and increased adhesion of JAK2-V617F positive granulocytes [31–33]. These findings suggest significant differences in the regulation of inflammation and pro-thrombotic risk between JAK2-V617F and *CALR*-mutated MPN patients.

Neutrophils are the most abundant leukocytes in the organism and therefore an important source of inflammatory cytokines. They are increasingly recognized as an important pathogenic link to chronic non-resolving inflammation and the pro-thrombotic risk in MPN [34–37]. MPN neutrophils display a malignant phenotype and contribute to a number of major pathological incidents in MPNs [34, 38]. Importantly, previous research has shown that JAK2-V617F positive neutrophils exhibit a pro-adhesive phenotype, which contributes to the marked pro-thrombotic state of JAK2-V617F positive MPN [39]. However, there is almost no data comparing the activities of *CALR*-mutated neutrophils versus JAK2-V617F positive neutrophils side-by-side in MPNs. Here, we

investigated a range of inflammatory conditions induced by neutrophil-specific expression of JAK2-V617F or CALRmut, which we hypothesized were related to patients' inflammatory symptoms and pro-thrombotic risks.

Materials and methods

Sex as a biological variable

Our study examined male and female animals, and similar findings are reported for both sexes.

Mouse models

The Ly6G-Cre JAK2-V617F mouse model was generated by crossing floxed heterozygous $JAK2^{+/loxP-VF-loxP}$ mice with $Ly6G^{+/Cre-tdTomato}Catchup^{IVM-red}$ mice. $JAK2^{+/loxP-VF-loxP}$ mice were kindly provided by Ann Mullally (Harvard Medical School, Boston, Massachusetts) [40]. Experiments were conducted using $JAK2^{+/loxP-VF-loxP}Ly6G^{+/Cre-tdTomato}Catchup^{IVM-red}(Ly6G-CreJAK2^{+/VF})$ and $JAK2^{+/+}Ly6G^{+/Cre-tdTomato}Catchup^{IVM-red}$ ($Ly6G-Cre JAK2^{+/+}$) mice as wild type (WT) controls [41]. Exon 1 of the *Ly6g*-gene was replaced by a knock-in allele of Cre recombinase and tdTomato leading to neutrophil-specific expression of JAK2-V617F. An additional Cre recombinase-dependence expression of tdTomato was achieved through a CAG promoter located in the *ROSA26* locus [41].

The Ly6G-Cre CALRdel mouse model was generated by crossing heterozygous mice harboring the loxP flanked CALRdel52 mouse-human chimeric oncogene in exon 9 ($CALR^{+/loxP-exon9-loxP}$) with Ly6G-Cre mice [42]. Experiments were conducted using $CALR^{+/loxP-exon9-loxP}Ly6G^{+/Cre-tdTomato}Catchup^{IVM-red}$ ($Ly6G-CreCALR^{+/del}$) and $CALR^{+/+}Ly6G^{+/Cre-tdTomato}Catchup^{IVM-red}$ ($Ly6G-Cre CALR^{+/+}$) mice as WT controls. Neutrophil-specific expression of CALRdel52 was induced by replacement of exon 1 of the *Ly6g*-gene by a knock-in allele of Cre recombinase and tdTomato. All mice used exhibited a CAG promoter-driven additional expression of tdTomato from the *ROSA26* locus in a Cre-dependent manner.

The Vav-Cre JAK2-V617F and CALRdel model have been described previously [42, 43].

Blood count analysis

Blood count analysis was obtained by an automatic blood counting machine (ADVIA 2120 systems, Siemens, Germany).

Flow cytometry analysis

Immunophenotyping by flow cytometry was performed using a FACSCanto II (BD Biosciences). Primary antibodies used are listed in Additional File 1: Table S1. Due to overlapping fluorescent spectra of tdTomato and

phycoerythrin (PE), PE-conjugated antibodies were not used in Ly6G-Cre mice.

Bone marrow and spleen sections

Hematoxylin-eosin staining was performed on bone marrow (BM) and spleen sections. After deparaffinization and rehydration, sections were stained with hematoxylin and eosin.

Analysis of hematopoietic stem and progenitor cells (HSPCs)

Isolating HSPCs and quantitative analysis was performed as previously described [43, 44].

Measurement of inflammatory cytokines

Cytokine concentrations in serum were determined by Eve Technologies, Canada (Mouse Cytokine Array/Che-mokine Array 32-Plex, duplicate testing) using two-fold diluted serum samples.

Metabolic flux analyses

Bioenergetics of neutrophils were recorded on a Seahorse XFe96 extracellular flux analyzer (Agilent Technologies, St. Clara, CA) as described previously [45, 46]. Details of the method are outlined in Additional file 2: Supplemental Methods.

In vitro time lapse recording of cell motility

BM cells were harvested from femur and tibia and neutrophils were isolated by negative selection [47] followed by fluorescence-activated cell sorting (FACS) using their tdTomato autofluorescence. Four wells of a 15-well angiogenesis μ -slide (Ibidi) were pre-coated overnight with ICAM-1 and VCAM-1 (5 μ g/mL, R&D Systems). Overall, 50,000 tdTomato expressing neutrophils were resuspended and seeded per well in 1xHBSS (Biochrom) containing 0.2% fatty acid-free BSA (Roth) and 1 mM HEPES (Life Technologies). The slide was subsequently transferred to the microscope stage in a 5% CO₂ atmosphere at 37 °C. Immediately after settling of the cells, time lapse recording was started using a Leica DMI6000 widefield microscope (40x objective; LAS AF software, version 2.0.2, Leica Microsystems, Germany). Brightfield and tdTomato fluorescence images were captured every 37 s in four wells at a time using automated XY-stage positioning over a period of one hour. Manual tracking of 50 cells per mouse was done with ImageJ (version v1.52n) and the ImageJ plugin MTrackJ (version 1.5.1).

Saphenous vein stenosis model

Partial ligation of the great saphenous vein (GSV) [48] was performed on 10 to 16 weeks old male Ly6G-Cre $JAK2^{+/VF}$ and $JAK2^{+/+}$ mice. Anesthetized mice (Ketamin 100 mg/kg bodyweight and Xylazine/Rompun 10 mg/kg

bodyweight) were fixated on the back on a 37 °C temperature-controlled heating pad. After removing the fur of the inner thigh, the GSV was microsurgically exposed under microscopic view (Leica S8 APO) and partially ligated using a 7–0 polypropylene suture. To avoid complete venous occlusion, a part of a needle tip (30 gauge; equivalent to a diameter of 0.255 mm) was inserted as placeholder and immediately removed after applying the partial ligation.

In vivo two-photon (2P) microscopy

In vivo two-photon (2P) microscopy was performed as previously described [49, 50] and is outlined in Additional file 2: Supplemental Methods.

Statistics

Statistical analysis was carried out using GraphPad Prism (version 9). Data are shown as mean ± SEM. Unpaired, two-tailed t-tests were applied. For comparison of gene expression between the $JAK2^{+/+}$ versus $JAK2^{+/VF}$ and $CALR^{+/+}$ versus $CALR^{+/del}$ groups of samples, the DESeq2 software was used.

Gene set enrichment analysis was performed using the GSEA v4.3.2 (UC San Diego and Broad Institute; <https://www.gsea-msigdb.org>). Comparisons exhibiting a p-value < 0.05 and FDR q-value < 0.15 were considered significant.

Results

Neutrophil-specific expression of *JAK2-V617F*, but not *CALRdel*, induces thrombocytosis and megakaryocyte hyperplasia

Aside from their crucial role in innate immunity, neutrophils have an important and previously underestimated function in the regulation of hematopoietic stem cell and erythropoietic niches in both normal physiologic conditions and MPN pathophysiology [51, 52]. To examine the effects of neutrophil-restricted expression of *JAK2-V617F* and of *CALRdel* in inflammation, Ly6G-Cre positive $JAK2^{+/VF}$, $JAK2^{+/+}$, $CALR^{+/del}$ and $CALR^{+/+}$ mice were generated as described under Material and Methods. Cre recombinase-dependent expression of tdTomato and of the transgene was achieved through a CAG promoter located in the *ROSA26* locus [41]. Control experiments demonstrated that *JAK2-V617F* or *CALRdel* is only expressed in tdTomato positive neutrophils of Ly6G-Cre $JAK2^{+/VF}$ and $CALR^{+/del}$ mice, respectively (Additional file 3: Fig. S1). The neutrophil-specificity of the Ly6G-Cre model (Catchup model) has been described previously [41]. Importantly, Ly6G-Cre directed tdTomato expression was absent in CD11b+Ly6G⁻ macrophages or other Ly6G⁻ leukocytes and in GMPs [41]. Additional control experiments in hematopoietic progenitors, in monocytes, in the erythrocyte lineage,

platelets and in megakaryocyte progenitors (MKPs) demonstrated almost complete tdTomato-negativity in Ly6G-Cre $JAK2^{+/VF}$ and Ly6G-Cre $CALR^{+/del}$ mice, respectively (Additional file 3: Fig. S2–4). In Ly6G-Cre $JAK2^{+/VF}$ and *CALRdel* ($CALR^{+/del}$) mice, white blood cell (WBC) counts and red blood cell (RBC) counts remained within the normal range (Fig. 1, A and D). However, there was a tendency towards an increase in neutrophil counts in $JAK2^{+/VF}$ mice, while hematocrit (HCT) and spleen weight tended to decrease in these mice (Fig. 1, B, C and E). Interestingly, there was a moderate but highly significant increase in PLT counts of $JAK2^{+/VF}$ mice ($JAK2^{+/VF}$: $1519 \pm 59 \times 10^9/L$; $JAK2^{+/+}$: $1146 \pm 58 \times 10^9/L$) in both male and female mice (Fig. 1F and Additional file 3: Fig. S5, A–C). Increased PLT counts were also observed in aged $JAK2^{+/VF}$ mice (Additional file 3: Fig. S5F). BM sections of $JAK2^{+/VF}$ mice exhibited megakaryocyte (MK) hyperplasia and formation of MK clusters, which are regarded as a hallmark of MPN [40, 53] (Fig. 1, G and I). Nonetheless, MK progenitor counts were comparable (Fig. 1H). Serum thrombopoietin (TPO) concentrations showed no discrepancies between the two mouse strains (Additional file 3: Fig. S5G). MK hyperplasia in $JAK2^{+/VF}$ mice was not caused by an increase in megakaryocyte/erythroid progenitors (MEP) in the BM (Additional file 3: Fig. S6A and C). Phenotypic analysis of HSPCs revealed that expression of *JAK2-V617F* or *CALRdel* in neutrophils did not result in any significant numerical or compositional changes of HSPCs in the BM or the splenic compartment (Additional file 3: Fig. S6, A–D). Additionally, examination of spleens did not reveal any discernible differences in spleen size or composition between both Ly6G-Cre $JAK2^{+/VF}$ and $CALR^{+/del}$ mice and their respective WT controls (Additional file 3: Fig. S7).

Neutrophil-specific expression of *JAK2-V617F*, but not *CALRdel*, up-regulates inflammatory cytokines in serum

A chronic non-resolving inflammatory syndrome with a pro-inflammatory cytokine signature in the serum is a significant disease feature in MPNs [54, 55]. However, the role of granulocytes in the inflammatory condition is not well-understood. To investigate whether expression of *JAK2-V617F* or *CALRdel* specifically in neutrophils induces pro-inflammatory cytokines, we measured serum concentrations of a panel of cytokines in Ly6G-Cre $JAK2^{+/VF}$ and $CALR^{+/del}$ mice (Fig. 2A). Compared to the WT controls, the cytokine levels of IL-1 α , IL-12 (p40), and M-CSF cytokines were significantly ($p < 0.05$) elevated in $JAK2^{+/VF}$ mice by factors of 1.8, 1.6 and 2.1, respectively (Fig. 2B and Additional file 1: Tab. S2). Furthermore, in Ly6G-Cre $JAK2^{+/VF}$ mice, although not statistically significant, levels of five additional cytokines in serum were observed to be upregulated by more than 1.5-fold: IL-1 β , IL-2, IL-10, IL-17, and TNF α (Additional

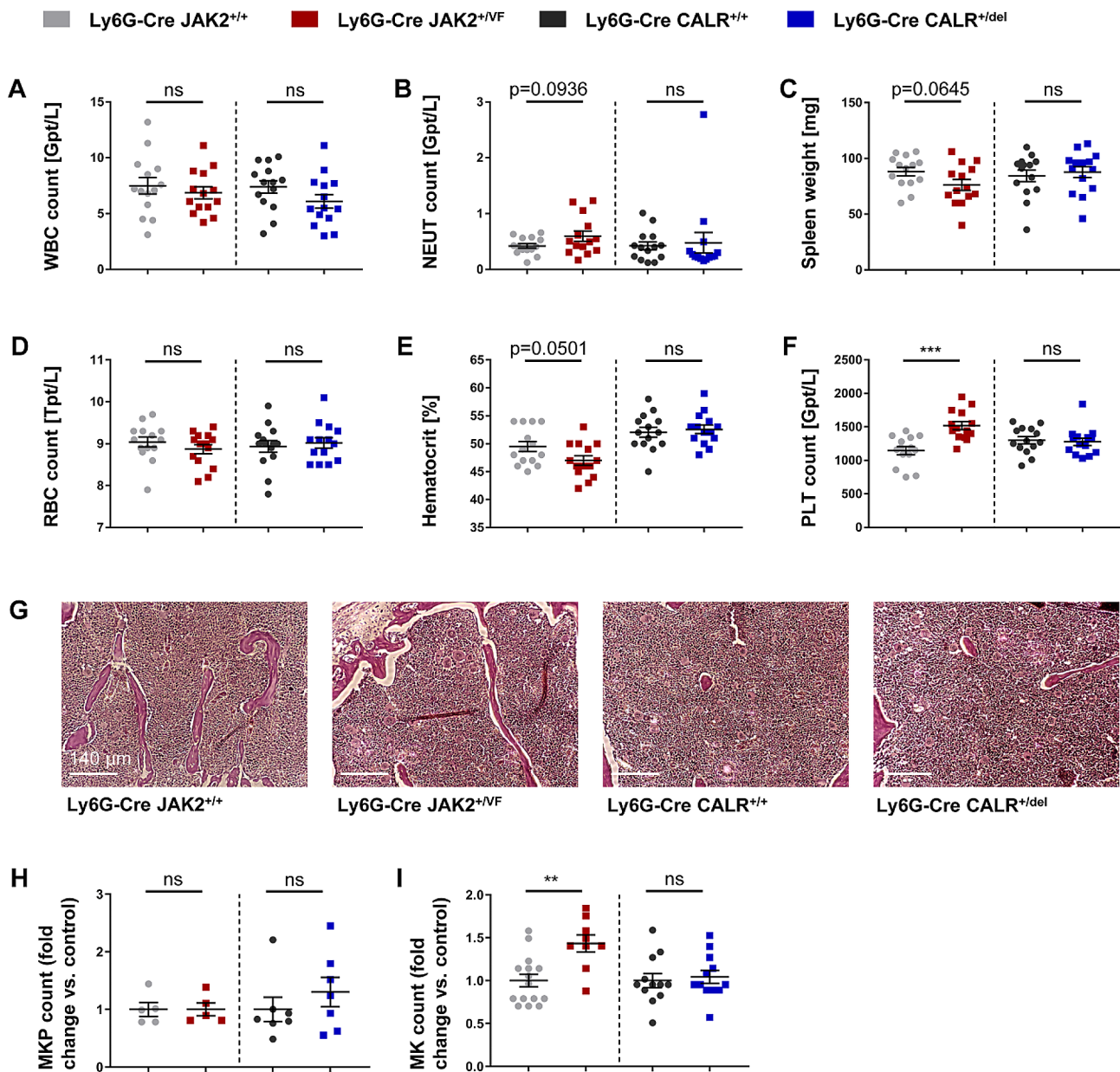


Fig. 1 Neutrophil-specific expression of *JAK2-V617F*, but not *CALRdel*, induces thrombocytosis and megakaryocyte hyperplasia. **(A-F)** White blood cell (WBC) count, neutrophil (NEUT) count, spleen weight, red blood cell (RBC) count, hematocrit, and platelet (PLT) count of Ly6G-Cre *JAK2*^{+/+}, *JAK2*^{+VF}, *CALR*^{+/+} and *CALR*^{+del} mice (each $n=14$). **(G)** Representative hematoxylin-eosin staining of bone marrow sections of *JAK2*^{+/+} ($n=5$), *JAK2*^{+VF} ($n=3$), *CALR*^{+/+} ($n=8$) and *CALR*^{+del} mice ($n=10$). **(H)** Megakaryocyte progenitor (MKP) counts in bone marrow of Ly6G-Cre *JAK2*^{+/+} ($n=5$), *JAK2*^{+VF} ($n=5$), *CALR*^{+/+} ($n=7$) and *CALR*^{+del} mice ($n=7$) shown as fold change versus control. **(I)** Quantitative analysis (performed in a blinded fashion) of megakaryocytes (MKs) in bone marrow of Ly6G-Cre *JAK2*^{+/+}, *JAK2*^{+VF}, *CALR*^{+/+} and *CALR*^{+del} mice in 200x high-power fields (HPF) showing numbers of MKs/HPF as fold change versus control. Data are shown as mean \pm SEM. ** $p \leq 0.01$, *** $p \leq 0.001$ (unpaired, two-tailed t-test)

file 1: Tab. S2). In contrast to the *JAK2-V617F* mutation, statistically significant changes in the serum cytokine levels were not induced by neutrophil-specific expression of *CALRdel* and levels of only two cytokines were up-regulated by more than 1.5-fold: IL-5 and LIX (CXCL5) (Additional file 1: Tab. S3). IL-5 has a significant role in type-2 adaptive immunity, which includes atopic diseases, but has not yet been implicated in cancer-associated

inflammation [56]. Together, this suggests that expression of *JAK2-V617F* in neutrophils is sufficient to induce typical MPN pro-inflammatory cytokines in serum [17–20]. Conversely, expression of *CALRdel* in neutrophils seems to have no significant impact on the induction of a pro-inflammatory cytokine signature in serum.

Recent studies revealed that IL-1 β has a pivotal role in clonal expansion, BM fibrosis and amplified

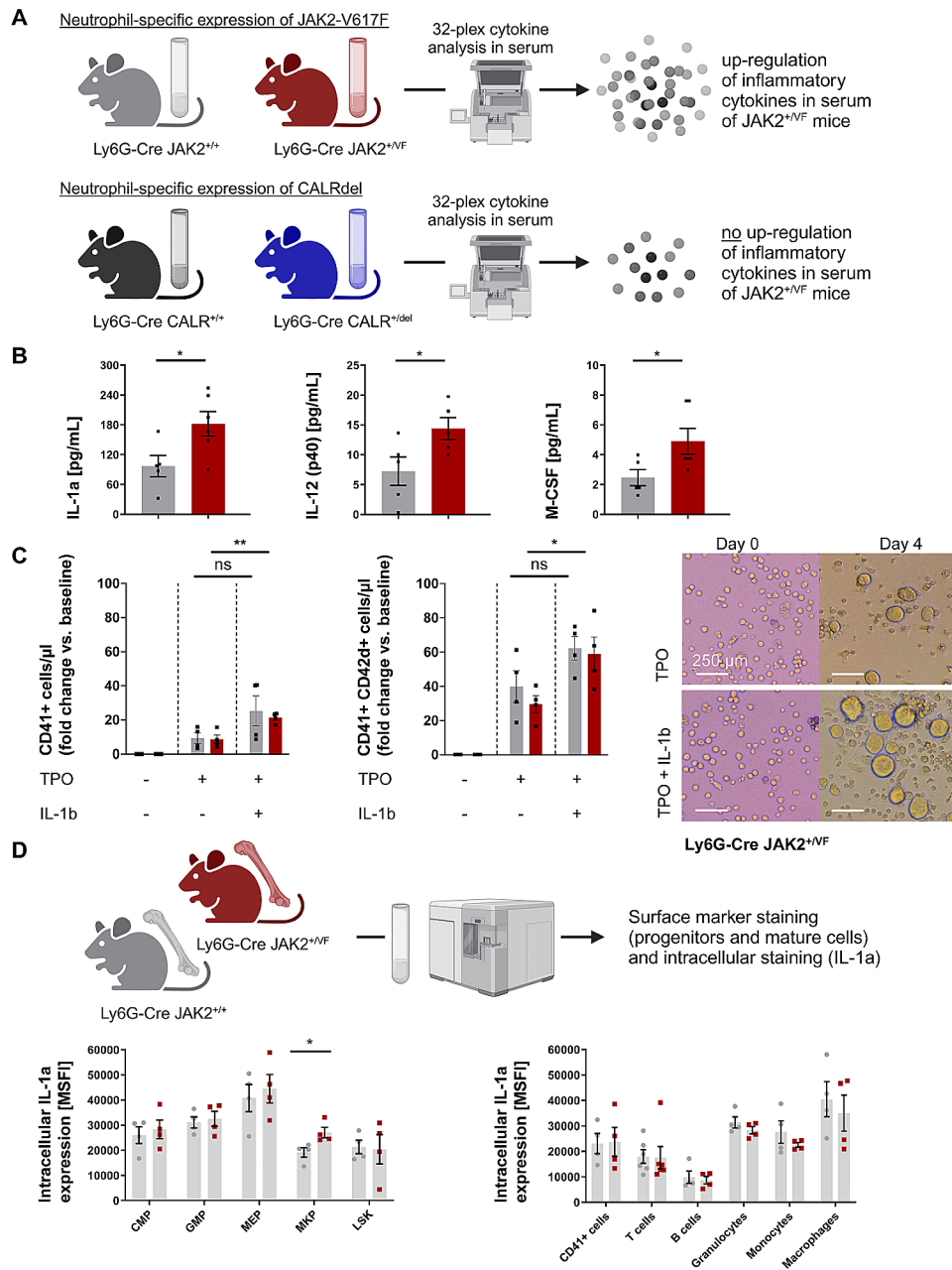
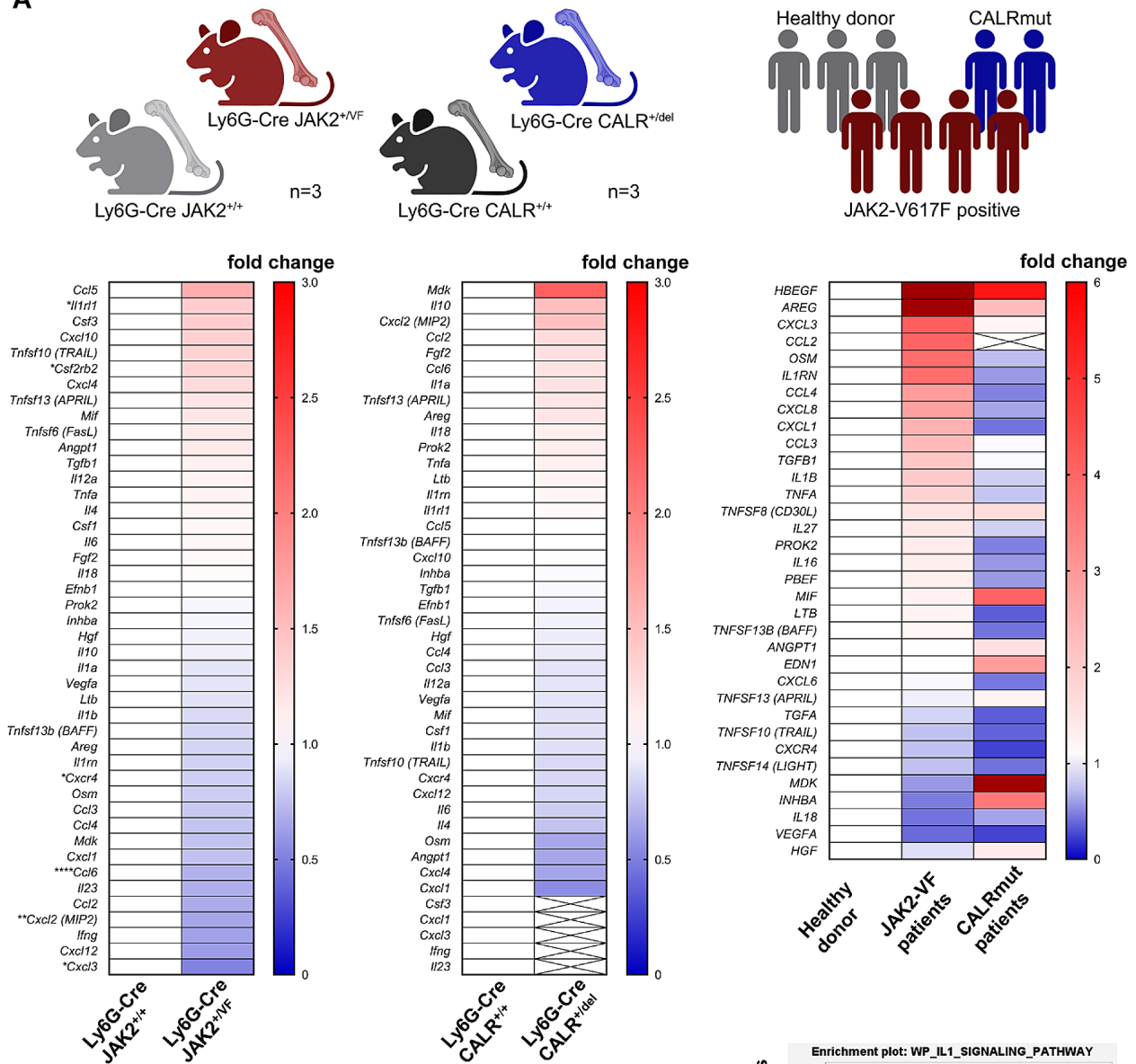


Fig. 2 Neutrophil-specific expression of *JAK2-V617F*, but not *CALRdel*, up-regulates inflammatory cytokines. **(A)** Cartoon depicting the experimental design to study serum cytokine concentrations in $JAK2^{+VF}$ and $CALR^{+del}$ mice in comparison to their corresponding WT controls. Cytokine protein concentrations in serum of Ly6G-Cre $JAK2^{+/+}$ ($n=6$) and $JAK2^{+VF}$ mice ($n=6$), and in serum of Ly6G-Cre $CALR^{+/+}$ ($n=8$) and $CALR^{+del}$ mice ($n=10$) were analyzed by Eve Technologies, Canada (Mouse Cytokine Array/Chemokine Array 32-Plex, duplicate testing). Created with Biorender.com. **(B)** Bar graphs of significantly elevated serum cytokine concentrations of IL-1 α , IL-12(p40) and M-CSF in Ly6G-Cre $JAK2^{+VF}$ mice. Data are shown as median \pm IQR. $*p \leq 0.05$ (unpaired, two-tailed t-test). **(C)** IL-1 β induced megakaryocytic differentiation of lineage-negative cells isolated from bone marrow. Left and middle panel: Impact of IL-1 β (25 ng/ml) on the number of formed immature (CD41 $^{+}$) and mature (CD41 $^{+}$ CD42d $^{+}$) megakaryocytes upon TPO-driven differentiation of lineage-negative cells isolated from bone marrow of Ly6G-Cre $JAK2^{+/+}$ and $JAK2^{+VF}$ mice (each $n=4$). Data are shown as mean \pm SEM. $*p \leq 0.05$ (unpaired, two-tailed t-test). Right panel: Representative images of megakaryocytes differentiated from lineage-negative bone marrow cells isolated from Ly6G-Cre $JAK2^{+/+}$ and $JAK2^{+VF}$ mice at baseline and upon four-day TPO-driven differentiation with or without IL-1 β ($n=2$). **(D)** Neutrophil-specific expression of *JAK2-V617F* increases IL-1 α expression in megakaryocyte progenitors (MKP). Intracellular staining for IL-1 α levels in various hematopoietic cell populations using anti-IL-1 α antibody and isotype control antibody was performed as described under Supplemental Methods. Mean fluorescence intensity (MFI) was measured by flow cytometry. The specific MFI (MSFI) was calculated by subtracting the MFI of the isotype control from the MFI of the anti-IL-1 α antibody stained sample. Data are shown as mean \pm SEM. $*p \leq 0.05$ (unpaired, two-tailed t-test with Welch correction). Cartoon created with Biorender.com

A



B

JAK2-VF patients vs. CALRmut patients

NES	Nominal p-value	FDR q-value	Gene set
1.73	<0.0001	0.09	IL-1 signaling pathway
1.58	<0.0001	0.10	IL-1 structural pathway
1.40	<0.0001	0.12	IL-1 receptor pathway

C

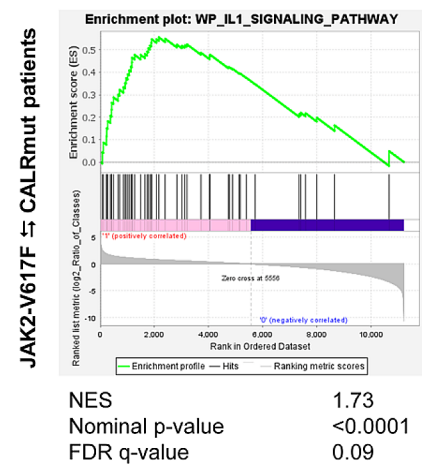


Fig. 3 (See legend on next page.)

(See figure on previous page.)

Fig. 3 RNA-seq in granulocytes from *JAK2-V617F* and *CALR-mutated* mice and patients shows distinct inflammatory cytokine signatures **(A)** Left and middle panel: RNA-seq of granulocytes obtained from Ly6G-Cre *JAK2^{+/+}*, *JAK2^{+VF}*, *CALR^{+/+}* and *CALR^{+del}* mice (each $n=3$) was performed by GENEWIZ Inc. (Leipzig, Germany). Using DESeq2, a comparison of gene expression between the *JAK2^{+/+}* versus *JAK2^{+VF}* and *CALR^{+/+}* versus *CALR^{+del}* groups of samples was performed. The heatmaps represent fold changes in mean normalized counts of cytokine RNA abundances relative to the WT controls. Left panel: Ly6G-Cre *JAK2^{+/+}* versus *JAK2^{+VF}* mice; middle panel: Ly6G-Cre *CALR^{+/+}* versus *CALR^{+del}* mice. *adjusted p -value ≤ 0.05 , **adjusted p -value ≤ 0.01 , ****adjusted p -value ≤ 0.0001 ; right panel: RNA-seq was performed on peripheral blood granulocytes isolated from *JAK2-V617F* positive ($n=4$), healthy donors ($n=3$) and *CALR-mutated* ($n=2$) patients by GENEWIZ Inc. (Leipzig, Germany). Using DESeq2, a comparison of RNA expression between *JAK2-V617F* positive patients versus age-matched healthy donors and *CALR-mutated* patients versus healthy donors was performed. The heatmaps depict fold changes of mean normalized counts of cytokine RNA abundances relative to the healthy donor controls. Cartoon created with Biorender.com. **(B)** GSEA of IL-1 pathways in granulocytes isolated from *JAK2-V617F* positive patients compared to *CALR-mutated* patients. Positive NES in the heatmap indicate substantial (FDR q -values < 0.15) enrichment in granulocytes from *JAK2-V617F* positive patients. The values point out NES for each pathway. All gene sets were obtained from the GSEA website (UC San Diego and Broad Institute; <https://www.gsea-msigdb.org>). **(C)** RNA-seq data from *JAK2-V617F* positive patients ($n=4$ consecutive patients) compared to *CALR-mutated* ($n=2$ consecutive patients) patients is tested for enrichment of genes related to the "Interleukin 1 Signaling Pathway" by Gene Set Enrichment Analysis (GSEA). GSEA was performed using the GSEAv4.3.2 (UC San Diego and Broad Institute; <https://www.gsea-msigdb.org>). Comparisons exhibiting a p -value < 0.05 and FDR q -value < 0.15 were considered significant. The enrichment map was used for visualization of the GSEA results. Normalized Enrichment Score (NES) and False Discovery Rate (FDR) p -values were calculated upon 10,000 gene set permutations

megakaryopoiesis associated with *JAK2-V617F*-driven MPN-like disease in mice [17, 18]. Both, the genetic deletion of IL-1 β and of IL-1R1, respectively and administration of anti-IL-1 β antibody and anti-IL-1R1 antibody, respectively suppressed increased PLT and BM CD41⁺ cell counts in *JAK2-V617F* driven MPN-mice [17, 18]. Therefore, we hypothesized that the higher PLT counts observed in the Ly6G-Cre *JAK2-V617F* model were due to the increased IL-1 β serum levels (Additional file 1: Tab. S2). Thus, we studied the impact of IL-1 β on the differentiation of lineage-negative (lin⁻) BM cells into MKs. Figure 2C displays that IL-1 β increased TPO-driven megakaryopoiesis in vitro using lin⁻ BM cells isolated from Ly6G-Cre *JAK2^{+/+}* and *JAK2^{+VF}* mice. Ploidy analysis additionally indicated an increase in 8 N-cells following IL-1 β stimulation (Supplementary Figure S8). Considering the published evidence [17, 18] regarding the significant role of IL-1 β in *JAK2-V617F*-induced thrombocytosis and elevated megakaryopoiesis, our findings support the concept that increased IL-1 β serum levels are responsible for the observed elevation of PLT and MK counts in Ly6G-Cre *JAK2^{+VF}* mice.

Next, we investigated which hematopoietic cell population is the source of the elevated serum levels of inflammatory cytokines in *JAK2-V617F* induced MPN-like disease. We focused on IL-1 α and performed intracellular IL-1 α staining in various hematopoietic cell types including hematopoietic progenitors. The results showed that granulocytes, B-cells, T-cells, monocytes and macrophages from Ly6G-Cre *JAK2^{+/+}* and *JAK2^{+VF}* mice expressed similar IL-1 α protein levels, respectively (Fig. 2D). However, MKP cells from Ly6G-Cre *JAK2^{+VF}* mice displayed significantly higher IL-1 α protein levels (Fig. 2D). Together, this data suggests that MKPs are a major source of the elevated IL-1 α serum levels in Ly6G-Cre *JAK2^{+VF}* mice. However, non-hematopoietic stromal cells may also participate in this process.

Cytokine gene expression signatures in *JAK2-V617F* and *CALRmut* neutrophils isolated from mice and humans

Next, we performed RNA-seq analysis on neutrophils isolated from Ly6G-Cre *JAK2^{+/+}*, *JAK2^{+VF}*, *CALR^{+/+}*, and *CALR^{+del}* mice. In *JAK2-V617F* neutrophils, 53 genes out of a total of 14,923 genes analysed were significantly (adjusted p -value < 0.05) regulated (Additional File 1, Tab. S6), whereas in *CALRdel* granulocytes no significant alteration were noted (data not shown). In order to determine whether the elevated cytokines observed in the serum of *JAK2-V617F* mice originated from *JAK2-V617F* granulocytes, the gene expression of a cluster of neutrophil-derived cytokines, previously reported by C. Tecchio, was examined [57]. The heatmap of relative changes induced by *JAK2-V617F* is depicted in Fig. 3A, left panel. Notably, four chemokine genes (*Cxcl2*, *Cxcr4*, *Cxcl3* and *Ccl6*) showed a statistically significant change (adjusted p -value < 0.05), whereas this signature was not present in neutrophils from *CALR^{+del}* mice (Fig. 3A, middle panel). In addition, *Il1r1* and *Csf2rb2* genes were also significantly (adjusted p -value < 0.05) regulated by *JAK2-V617F*, but not by *CALRdel*. This data suggests that the up-regulation of inflammatory cytokines in serum of Ly6G-Cre *JAK2^{+VF}* mice (IL-1 α , IL-12 (p40), and M-CSF) does not derive directly from *JAK2-V617F* neutrophils. Instead, indirect mechanisms are involved employing other hematopoietic and possibly non-hematopoietic cells. An example for this is the IL-1 α production in MKPs illustrated in Fig. 2D. Potentially this is regulated via signals from the above mentioned chemokine signature (*Cxcl2*, *Cxcr4*, *Cxcl3* and *Ccl6*), which needs to be further investigated. Regarding the mechanism of action of *CALRdel* in neutrophils, it is worth mentioning that polymorphonuclear cells (PMN) were reported to express low levels of the TPO receptor c-Mpl and that TPO transiently induces low level STAT1 tyrosine phosphorylation in granulocytes [58]. Additionally, Terada and colleagues [59] found that TPO stimulates ex vivo expansion of

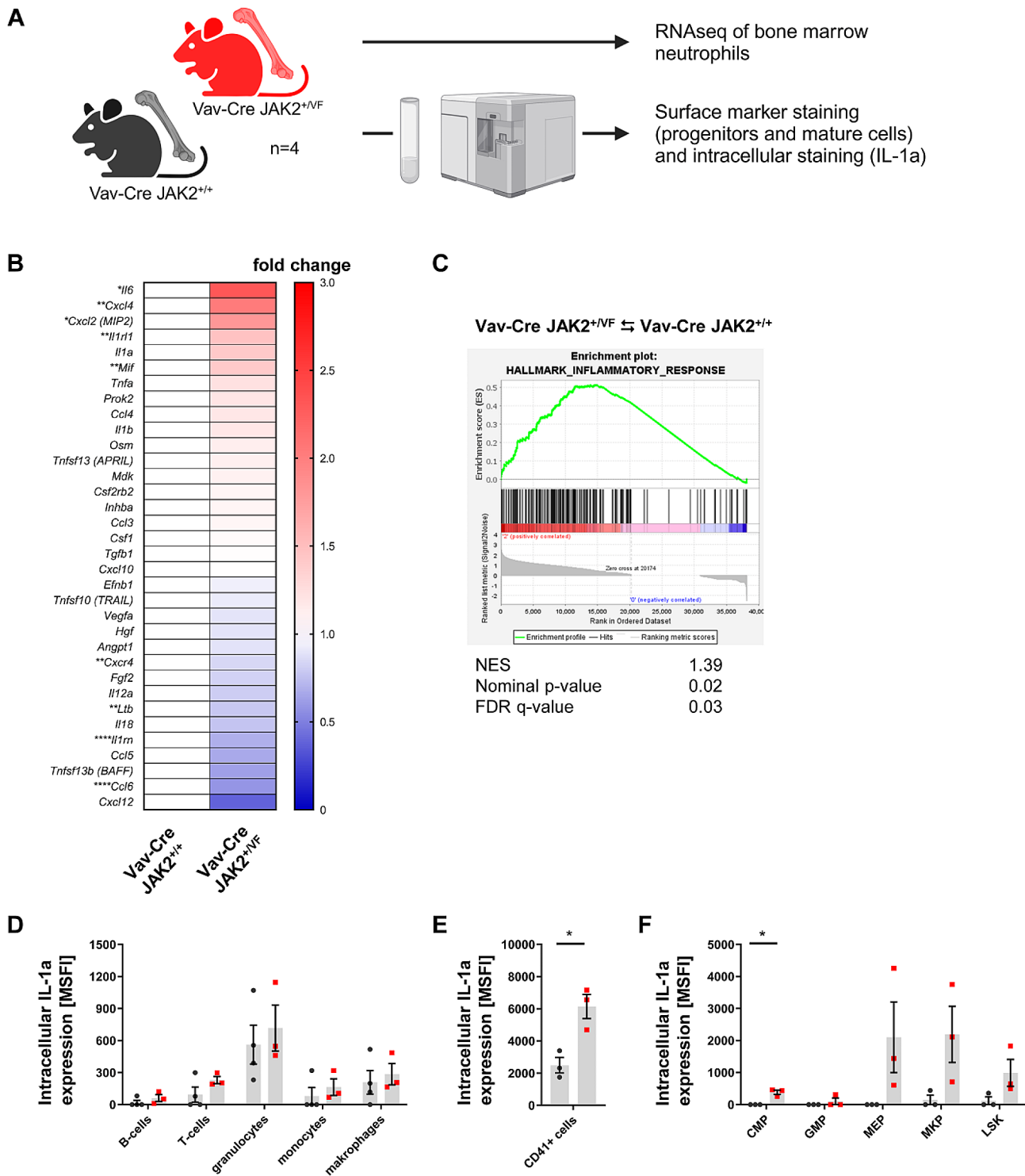


Fig. 4 (See legend on next page.)

neutrophils during the early stages of differentiation. Thus, the available literature suggests that neutrophils or a fraction of neutrophils possess functional MPL, indicating that mutated CALR may bind to MPL thereby exhibiting its oncogenic functions. Therefore, we investigated

MPL expression on BM-derived neutrophils in our CAL-Rmut model. FACS analysis of BM-derived neutrophils of Ly6G-Cre *CALR*^{+/+} and *CALR*^{+/del} mice detected low level MPL expression (Additional file 3: Fig. S9A). Furthermore, following incubation with TPO, a slight

(See figure on previous page.)

Fig. 4 Pan-hematopoietic expression of *JAK2-V617F* up-regulates pro-inflammatory cytokines in neutrophils and hematopoietic progenitors **(A)** Cartoon depicting the experimental design to study gene expression signatures in neutrophils and intracellular IL-1 α expression in Vav-Cre *JAK2^{+VF}* mice in comparison to their corresponding WT controls. Created with Biorender.com. **(B)** RNA-seq of granulocytes obtained from Vav-Cre *JAK2^{+VF}* and *JAK2^{+/+}* mice (each $n=4$) was performed by GENEWIZ Inc. (Leipzig, Germany). Using DESeq2, a comparison of gene expression between the Vav-Cre *JAK2^{+/+}* versus *JAK2^{+VF}* groups of samples was performed. The heatmaps represent fold changes in mean normalized counts of cytokine RNA abundances relative to the WT controls. Vav-Cre *JAK2^{+/+}* versus *JAK2^{+VF}* mice; *adjusted p-value ≤ 0.05 , **adjusted p-value ≤ 0.01 , ****adjusted p-value ≤ 0.0001 **(C)** GSEA of “Hallmark Inflammatory Response” genes in granulocytes isolated from Vav-Cre *JAK2^{+VF}* and *JAK2^{+/+}* mice. The enrichment map was used for visualization of the GSEA results. Normalized Enrichment Score (NES) and False Discovery Rate (FDR) p-values were calculated upon 10,000 gene set permutations. The positive NES of 1.39 in the figure indicates substantial (FDR q-value = 0.03; nominal p-value = 0.02) enrichment in genes linked with the inflammatory response. The “Hallmark Inflammatory Response” gene set was obtained from the GSEA website (UC San Diego and Broad Institute; <https://www.gsea-msigdb.org>). **(D, E, F)** Intracellular staining for IL-1 α levels in various hematopoietic cell populations using anti-IL-1 α antibody and isotype control antibody, respectively was performed as described under Supplemental Methods. Mean fluorescence intensity (MFI) was measured by flow cytometry. The specific MFI (MSFI) was calculated by subtracting the MFI of the isotype control from the MFI of the anti-IL-1 α antibody stained sample. Data are shown as mean \pm SEM. * $p \leq 0.05$ (unpaired, two-tailed t-test with Welch correction)

increase of p-STAT5 was observed in the neutrophils of Ly6G-Cre *CALR^{+del}* mice (Additional file 3: Fig. S9B). However, CALRdel is able to activate the G-CSFR as demonstrated by Chachoua et al. [8]. Therefore, CALRdel may dysregulate intrinsically some processes in granulocytes via its action on G-CSFR.

In order to compare cytokine gene expression in granulocytes obtained from healthy donors with *JAK2-V617F* and CALR mutant patients (clinical characteristics are depicted in Additional file 1: Tab. S4), we performed RNA-seq and generated a heatmap of cytokine gene expression in human neutrophils (Fig. 3A, right panel). Apparently, the fold-changes were more prominent as compared to the Ly6G-Cre mouse models (Fig. 3A, left and middle panel). However, when considering the adjusted p-values the changes in gene expression were not statistically significant. This is not unexpected, because there is high inter-individual variability which is influenced, among other factors, by inherited genetic predisposition factors and disease phenotype. Nevertheless, the overall observed changes high-lighted differences between the two groups of patients investigated (Fig. 3A, right panel): generally, *JAK2-V617F* positive patients displayed a greater number of upregulated cytokines in comparison to those carrying CALR mutations, where more cytokines were downregulated. Interestingly, in comparison to healthy donors *CXCL3*, *CCL2*, *CCL4*, *CXCL8*, *CXCL1*, and *CCL3* showed up-regulation in *JAK2-V617F* positive patients, whereas these genes were unchanged or down-regulated in CALR mutant patients (Fig. 3A, right panel). Furthermore, gene expression of *IL1RN*, *IL1B*, and *TNFA* also displayed up-regulation in *JAK2-V617F* patients, whereas in CALR-mutant patients they showed a tendency to decrease (Fig. 3A, right panel). This data is interesting, given the crucial role of IL-1 β in the development of *JAK2-V617F* positive disease [17, 18]. However, it requires further analysis in a larger cohort of patients.

To investigate whether we could differentiate between *JAK2-V617F* and CALR mutant patients based on gene expression profiling, we aimed to determine if there

were any differentially expressed functional pathways. We hypothesized that IL-1 signaling could be an interesting candidate based on previously published results [17, 18] and on the increase in gene expression of *IL1B* in neutrophils of *JAK2-V617F* positive patients (Fig. 3A, right panel). Importantly, Gene Set Enrichment Analysis (GSEA) [60, 61] revealed a remarkable and highly significant enrichment of the “Interleukin 1 Signaling Pathway”, “IL-1 Structural Pathway” and “IL-1R Pathway” in neutrophils sampled from patients with *JAK2-V617F*, when compared with CALR-mutated patients (Fig. 3B and C). Analysis of *JAK2-V617F* positive patients versus healthy donors also indicated a trend towards an enrichment of these pathways (Additional file 1: Tab. S5). Together, this data portrays a marked influence of the *JAK2-V617F* mutation in generating an IL-1 response profile in granulocytes of MPN patients.

Pan-hematopoietic expression of *JAK2-V617F* induces a prominent inflammatory cytokine signature in neutrophils

Unlike in the Ly6G-Cre *JAK2^{+VF}* model, granulocytes in Vav-Cre *JAK2^{+VF}* mice interact with signals from various other *JAK2-V617F* positive cell populations (such as progenitor cells, MKs, endothelial cells, etc.). This interaction potentially leads to more significant differences in gene expression, compared to the more subtle changes seen in granulocytes from Ly6G-Cre *JAK2^{+VF}* mice. The Vav-Cre *JAK2^{+VF}* mouse model has been previously described and reliably recapitulates a PV-like phenotype of MPN [40, 43]. Neutrophils from Vav-Cre *JAK2^{+VF}* and *JAK2^{+/+}* mice were isolated and RNA-seq was performed (Fig. 4A). 3,508 genes out of a total of 13,881 genes were significantly (adjusted p-value < 0.05) regulated in neutrophils from Vav-Cre *JAK2^{+VF}* mice (data not shown). In comparison to the low number of regulated genes in the Ly6G-Cre *JAK2^{+VF}* model, this indicates that the gene expression signature of neutrophils in *JAK2-V617F* induced disease is not primarily regulated by cell-intrinsic *JAK2-V617F* expression. Instead, *JAK2-V617F* neutrophils are more sensitive to extrinsic signals originating from other *JAK2-V617F* positive hematopoietic cells.

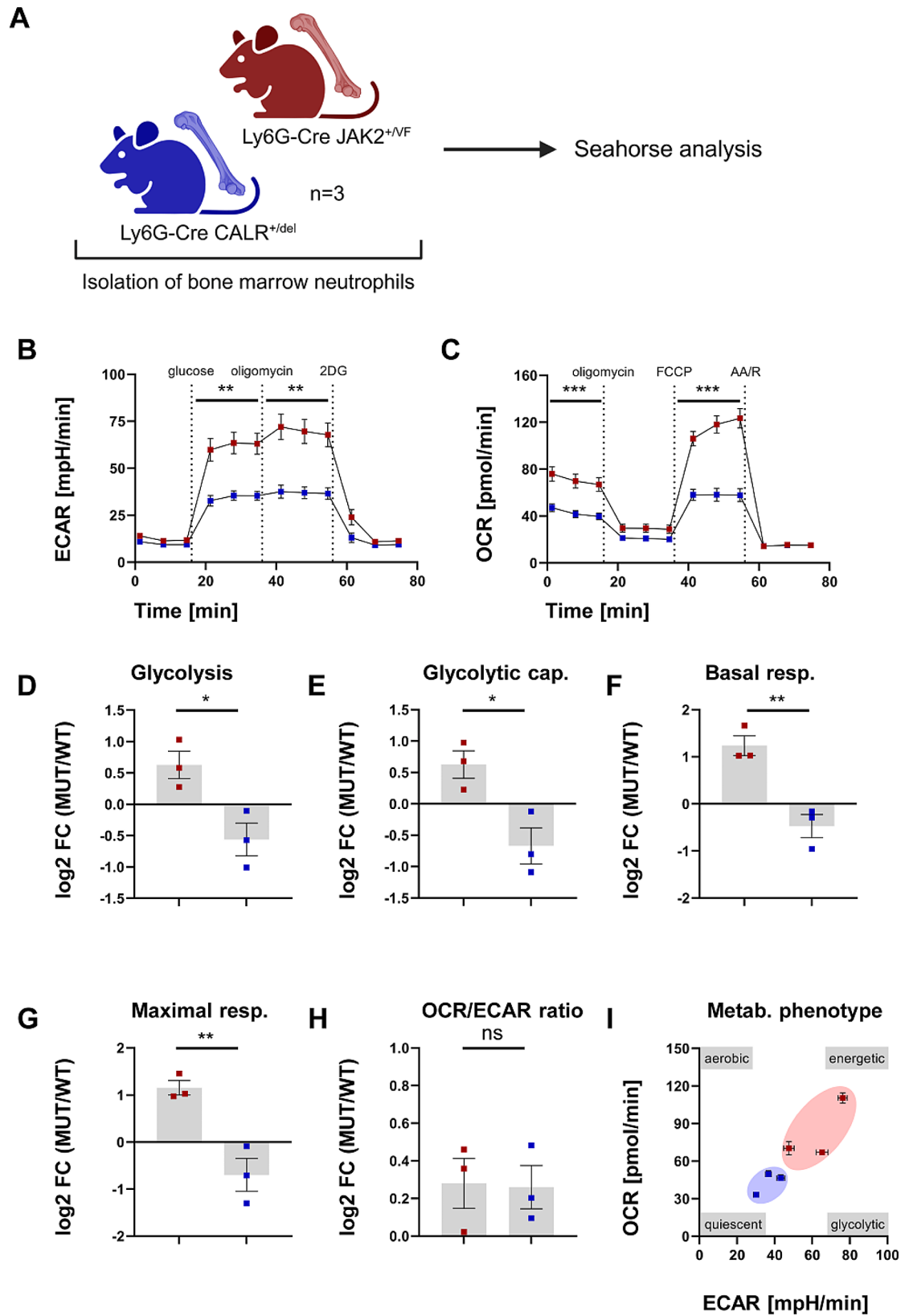


Fig. 5 (See legend on next page.)

(See figure on previous page.)

Fig. 5 Neutrophils isolated from Ly6G-Cre *JAK2^{+VF}* mice display enhanced metabolic activity. **(A)** Cartoon depicting the experimental design to study metabolic activity in neutrophils isolated from Ly6G-Cre *JAK2^{+VF}* and *CALR^{+del}*. Created with Biorender.com. **(B)** Glycolysis stress test (GST) and **(C)** mitochondrial stress test (MST) analyzing extracellular acidification rate (ECAR), as a surrogate for aerobic glycolysis, and oxygen consumption rate (OCR), as a surrogate for oxidative phosphorylation in neutrophils isolated from Ly6G-Cre *JAK2^{+VF}* and Ly6G-Cre *CALR^{+del}* ($n = 3$ with 3–6 technical replicates) were recorded in real-time upon sequential injection of compounds/inhibitors as described in the Supplemental Methods. The data presented were normalized to the background (phase 1 for GST and phase 4 for MST). Based on these and the corresponding wild-type data (Supplemental Fig. 7A and B), the metabolic parameters glycolysis **(D)**, glycolytic capacity **(E)**, basal respiration **(F)**, maximal respiration **(G)**, and the OCR/ECAR ratio as a surrogate for the balance between glycolysis and OXPHOS **(H)** were calculated and presented as the log₂ fold change (log₂ FC) of each individual relative to the respective wild-type average. **(I)** The baseline overall metabolic phenotype was calculated from **(B)** and **(C)** and plotted as an ECAR/OCR map. Data are shown as mean \pm SEM. * $p \leq 0.05$, ** $p \leq 0.01$, *** $p \leq 0.001$ (unpaired, two-tailed t-test). Abbreviations: OCR, oxygen consumption rate; ECAR, extracellular acidification rate; 2DG, 2-deoxyglucose; FCCP, Carbonyl cyanide-p-trifluoromethoxyphenylhydrazone; AA/R, Antimycin A/Rotenone

Next, we focused on the cytokine gene expression levels induced by JAK2-V617F and generated a heatmap of relative changes (Fig. 4B). Significant changes (adjusted p -values < 0.05) were detected in nine genes by DESeq2 analysis. *Il6* (2.3-fold change), *Cxcl4* (2.0-fold change), *Cxcl2* (1.8-fold change), *Il1rl1* (1.4-fold change) and *Mif* (1.4-fold change) were identified as the five up-regulated cytokine genes in JAK2-V617F positive neutrophils, while *Cxcr4* (0.8-fold change), *Ltb* (0.7-fold change), *Il1rn* (0.6-fold change) and *Ccl6* (0.58-fold change) showed a decrease. These changes in gene expression did not overlap with the panel of upregulated cytokines in serum of Vav-Cre *JAK2^{+VF}* mice which comprises CCL2, CCL11, CXCL5, CXCL9, CXCL10 and IL-1 α (as published previously [43]), again suggesting that neutrophils are not the primary cellular source of upregulated serum cytokines in JAK2-V617F induced disease.

Since neutrophils are recognized as an important pathogenic link to inflammation we performed Gene Set Enrichment Analysis (GSEA) on RNA-seq data from neutrophils of Vav-Cre *JAK2^{+VF}* and *JAK2^{+/+}* mice utilizing the “Hallmark Inflammatory Response” signature from the Molecular Signature Database (MSigDB) hallmark gene set collection [62] (Fig. 4C). GSEA indicated a highly significant enrichment of genes linked to “Hallmark Inflammatory Response” in neutrophils from Vav-Cre *JAK2^{+VF}* mice (Fig. 4C). Of note, this signature was not enriched in neutrophils obtained from Ly6G-Cre *JAK2^{+VF}* mice (data not shown). Based on this data, we conclude that the inflammatory gene expression signature of JAK2-V617F neutrophils is particularly prone to external signals originating from other JAK2-V617F positive cells.

Next, we examined which hematopoietic cell populations are the source of the elevated serum levels of inflammatory cytokines in the Vav-Cre *JAK2-V617F* model. We focused on IL-1 α (upregulated by a factor of 4.8 in serum of Vav-Cre *JAK2^{+VF}* mice) and performed intracellular IL-1 α staining in various hematopoietic cell types including hematopoietic progenitors. The results showed that granulocytes, B-cells, T-cells, monocytes and macrophages from Vav-Cre *JAK2^{+/+}* and *JAK2^{+VF}* mice expressed similar IL-1 α protein levels,

respectively (Fig. 4D). However, CD41⁺ cells from Vav-Cre *JAK2^{+VF}* mice displayed significantly higher IL-1 α protein levels (Fig. 4E). Elevated IL-1 α levels were also found in CMP (Fig. 4F). MEP, MKP and LSK cells from Vav-Cre *JAK2^{+VF}* mice also trended in this direction (Fig. 4F). Together, this data suggests that MKs and myeloid progenitors but not granulocytes are major contributors to the elevated IL-1 α serum levels in Vav-Cre *JAK2^{+VF}* mice. However, in myelofibrosis, it has been shown that both, myeloid progenitors and mature myeloid cells, may produce inflammatory cytokines, yet with distinct cytokine secretion profiles [63].

Neutrophil-specific expression of JAK2-V617F and CALRdel, respectively differentially affects the metabolic activity

It is well established that an inflammatory phenotype of immune and tissue-resident cells is reflected by, if not dependent on, an altered cellular metabolism for meeting the cells' increased metabolic demands [45, 46]. Therefore, we compared the metabolic profile of neutrophils isolated from Ly6G-Cre *JAK2^{+VF}* and *CALR^{+del}* mice by means of real-time metabolic flux analyses (Fig. 5A). Neutrophils from *JAK2^{+VF}* mice displayed an overall increased metabolic activity (Fig. 5B-G). Both the glycolytic (Fig. 5B) as well as the respiratory (Fig. 5C) parameters tested were significantly higher compared to the neutrophils isolated from Ly6G-Cre *CALR^{+del}* mice. When compared to the respective wild type controls (Additional file 3: Fig. S10A and B), the metabolic parameters glycolysis (Fig. 5D), glycolytic capacity (Fig. 5E), basal respiration (Fig. 5F), maximal respiration (Fig. 5G), revealed higher activity in JAK2-V617F neutrophils and less activity in CALRdel neutrophils. Additional metabolic parameters are depicted in Additional file 3: Fig. S10 and are in line with these results. The OCR/ECAR ratio (Fig. 5H) as a surrogate for the balance between glycolysis and OXPHOS was similarly increased in both genotypes. However, the baseline overall metabolic phenotype (Fig. 5I) plotted as an ECAR/OCR map displayed a clear segregation between JAK2-V617F and CALRdel neutrophils with a more energetic profile for the former and a more quiescent profile for the latter. Thus, it appears that the higher inflammatory activity of

JAK2-V617F neutrophils as characterized by the marked pro-inflammatory cytokine profiles described above is mirrored by a striking increase in the metabolic activity. It will be interesting to test this hypothesis in future studies by using inhibition experiments. Additional metabolic parameters including comparisons of the respective WT controls and the comparisons between JAK2-V617F versus WT and CALRdel versus WT are shown in Additional file 3: Fig. S10.

Neutrophil-specific expression of JAK2-V617F, but not CALRdel, decreases migration of granulocytes in vitro

Inflammatory conditions cause granulocytes to be sequestered from the circulation and directed towards the endothelial layer of blood vessels via the leukocyte adhesion cascade process [64, 65]. Cell migration of granulocytes on the endothelium is a multi-faceted biological process that relies heavily on molecular communication between integrin receptors LFA-1 and VLA-4 and their corresponding ligands, ICAM-1 and VCAM-1, along with integrin outside-in signaling and cytoskeletal re-organization that prompts actin polymerization (for reviews, see Guenther-C [65], De Pascalis & Etienne-Manneville [66] and Nourshargh & Alon [67]). Both VLA-4 - VCAM-1 and LFA-1 - ICAM-1 interactions play significant roles in regulating neutrophil adhesion and leukocyte-vessel wall interactions [67]. Therefore, we investigated cell migration of granulocytes on VCAM-1 and ICAM-1 coated surfaces (Fig. 6A). To accurately quantify cell movement, we considered the parameters which are visually represented in Fig. 6B: accumulated distance, displacement from origin, mean velocity (speed) and directness of migration (directness index). Neutrophils obtained from Ly6G-Cre *JAK2^{+VF}* mice demonstrated a significant decrease in both accumulated distance (85% of WT control) and displacement from origin (68% of WT control) as shown in Fig. 6, C and D and in Additional file 1: Tab. S7. Significantly, no notable differences in these parameters were found in *CALR^{+del}* mice (Fig. 6, G and H and Additional file 1: Tab. S6). Additionally, the mean velocity of JAK2-V617F positive neutrophils was noticeably lower (at 85% of WT control) (Fig. 6E and Additional file 1: Tab. S7), whereas no variations were observed in the CALRdel model (Fig. 6I and Additional file 1: Tab. S7). Finally, the mean directness index indicating the directed migration of JAK2-V617F positive neutrophils from their origin to their final position was diminished to 79% of the corresponding WT control group (Fig. 6F and Additional file 1: Tab. S7). Again, no significant differences were observed in CALRdel compared to CALR-WT neutrophils (Fig. 6J and Additional file 1: Tab. S7). These data indicate a significant decrease in the migratory capacity of neutrophils expressing JAK2-V617F, but not of those

expressing CALRdel. As a consequence, this may translate into pronounced accumulation of JAK2-V617F neutrophils at the site of an inflamed environment in vivo.

Partial ligation of the saphenous vein demonstrates reduced migration of JAK2-V617F positive neutrophils in vivo

To examine neutrophil migration on the endothelium in an inflamed vessel in vivo, we utilized intravital 2P microscopy of neutrophils in Ly6G-Cre *JAK2^{+VF}* mice after partially ligating the great saphenous vein (GSV) which provokes an inflammatory condition (Fig. 7A and B). Notably, we found a general decline of migration parameters in line with the in vitro observation: a decrease in the accumulated distance to 80% and a decrease in the mean displacement to 93% of the WT controls in the detected tracks of JAK2-V617F positive neutrophils (Fig. 7, C and D and Additional file 1: Tab. S7).

Additionally, JAK2-V617F neutrophils migrated significantly slower than JAK2-WT cells, with a mean velocity reduced to 79% of the WT control (Fig. 7E and Additional file 1: Tab. S7). However, the mean directness index of JAK2-V617F positive neutrophils in vivo was higher (125%) as compared to the WT group (Fig. 7F and Additional file 1: Tab. S7). The increased directness index indicates that despite their slower speed, JAK2-V617F neutrophils migrate in a more direct manner from their origin to their end position across the endothelium of an inflamed vessel. Moreover, we observed that cell sphericity in the JAK2-V617F neutrophils was higher than in the WT controls, suggesting enhanced rolling and adhesion of intravascular cells at the endothelium (Fig. 7G). Analysis of the only cell fraction with high sphericity (i.e. above the median sphericity of all tracks) showed a strong decrease in mean velocity in the JAK2-V617F neutrophils, indicating that these cells were rolling slower on the vascular endothelium than WT controls (Fig. 7H). Therefore, increased rolling and tethering, reduced accumulated distance and enhanced directness of cell movement in vivo may result in increased gathering of JAK2-V617F positive neutrophils at the inflamed endothelium site, ultimately contributing to the pro-thrombotic state of JAK2-V617F positive disease. Using intravital 2P-microscopy, we have shown previously [69] that inhibition of integrin VLA4 expressed on granulocytes strongly impacts the mobility of granulocytes in vessels.

Expression of JAK2-V617F and CALRdel, respectively re-programs the binding characteristics to ICAM-1, VCAM-1 and selectins in neutrophils

Leukocyte migration on the endothelium employs the mesenchymal migration mode and relies heavily on

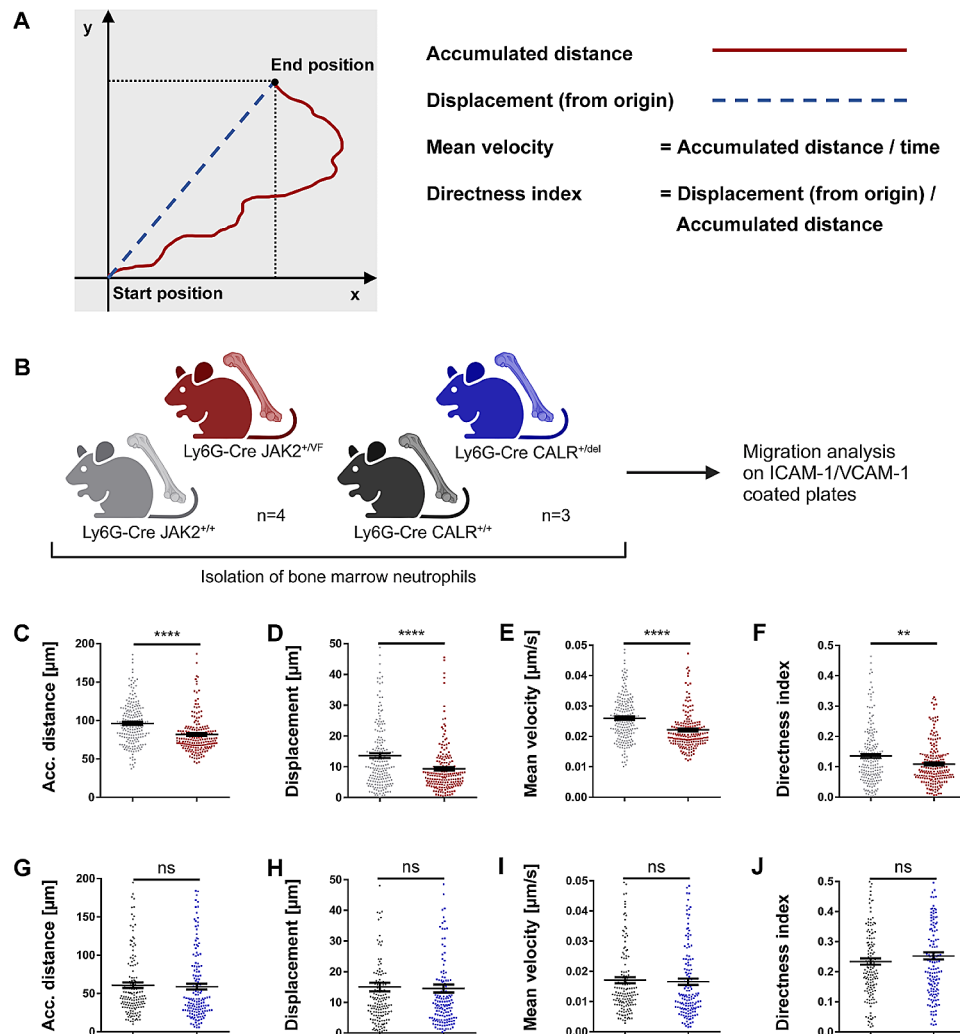


Fig. 6 Neutrophil-specific $JAK2$ -V617F, but not $CALR^{del}$, changes the migration behavior of neutrophils in vitro. **(A)** Scheme of cell migration parameters investigated. (adapted from Zengel et al.; [68]. Accumulated distance from origin to end position is indicated as a red line. Displacement as minimum distance between origin and end position is depicted with the blue dashed line. Mean velocity is calculated from the ratio of accumulated distance and time. Directness as ratio of displacement and accumulated distance indicates a measure of how direct a cell migrates from its origin to its end position. A directness value tending towards 1 indicates a straight migration from the start to the end position. Thus, an increase in directness index indicates that cells more directly migrate from their origin to their end position. **(B)** Cartoon depicting the experimental design to study migration characteristics in neutrophils isolated from Ly6G-Cre $JAK2^{+/VF}$ and $CALR^{+/del}$ mice in comparison to their corresponding WT controls. Created with Biorender.com. **(C-F)** Microfluidic chambers were coated with recombinant mouse ICAM-1 and VCAM-1. tdTomato expressing neutrophils isolated from Ly6G-Cre $JAK2^{+/VF}$ and $JAK2^{+/+}$ mice were seeded and time lapse recording of cell migration was started. Neutrophils isolated (200 tdTomato⁺ neutrophils investigated) from Ly6G-Cre $JAK2^{+/+}$ and $JAK2^{+/VF}$ mice (each $n=4$) exhibited the following migration parameters: accumulated distance of 96.2 μm compared to 81.9 μm , displacement of 13.6 μm compared to 9.3 μm , mean velocity of 0.026 $\mu\text{m}/\text{sec}$ compared to 0.022 $\mu\text{m}/\text{sec}$, and directness index of 0.14 compared to 0.11. **(G-J)** Migration parameters obtained in 150 tdTomato⁺ neutrophils investigated in Ly6G-Cre $CALR^{+/+}$ and $CALR^{+/del}$ mice (each $n=3$). Data are shown as mean \pm SEM. ** $p \leq 0.01$, **** $p \leq 0.0001$ (unpaired, two-tailed t-test)

integrins [65]. Previous studies have suggested that increased binding of integrin receptors to their ligands negatively affects cell motility [70, 71]. Therefore, we investigated the activation of $\beta 1$ and $\beta 2$ integrins and of selectins in neutrophils derived from Ly6G-Cre $JAK2^{+/VF}$ and $CALR^{+/del}$ mice (Fig. 8A). The expression levels of CD18 ($\beta 2$ integrin chain present in LFA1), CD29 ($\beta 1$ integrin chain present in VLA4) and CD162 (PSGL-1, which binds to E- and P-selectin) were found

to be unchanged (Fig. 8, B-D). On neutrophils, VLA-4 and LFA-1 are the primary $\beta 1$ and $\beta 2$ integrins that bind to VCAM-1 and ICAM-1, respectively. Static adhesion of neutrophils from Ly6G-Cre $JAK2^{+/VF}$ and $CALR^{+/del}$ mice to ICAM-1-coated plates was comparable to that of their WT counterparts (Fig. 8E). However, tdTomato⁺ neutrophils from Ly6G-Cre $JAK2^{+/VF}$ mice exhibited a slightly but significantly increased static adhesion to VCAM-1-coated surfaces (Fig. 8F). However, there

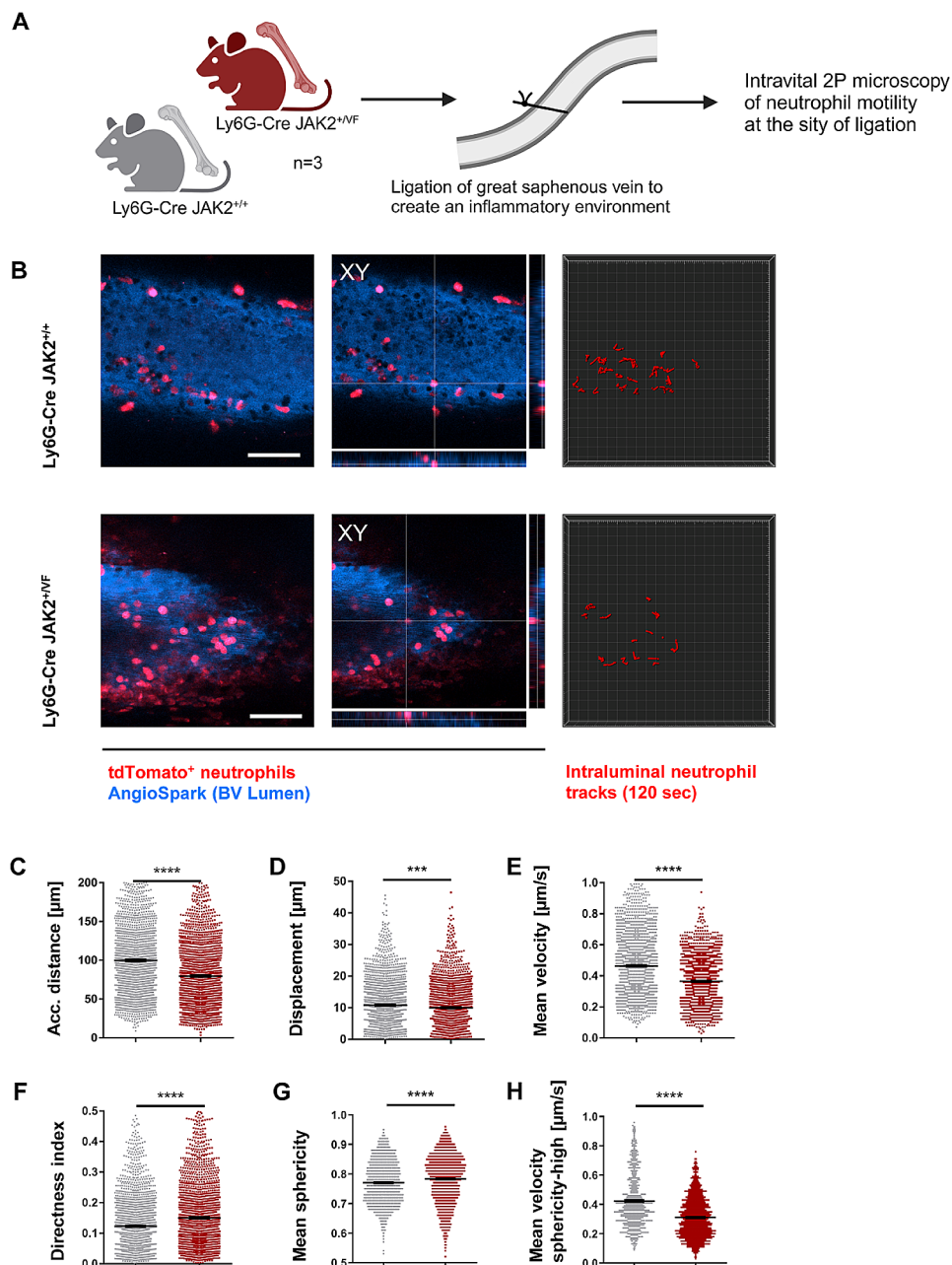


Fig. 7 *JAK2-V617F* suppresses the motility of neutrophils in an inflammatory environment. **(A)** Cartoon depicts experimental design to investigate neutrophil intraluminal crawling after partial ligation of the great saphenous vein (GSV) using intravital 2P microscopy. Created with Biorender.com. **(B)** To identify neutrophils (red) within the GSV from those localized in the surrounding connective tissue, AngioSPARK680 (blue) was applied intravenously. Imaging was started 20 min after applying partial ligation of the GSV, two examples from imaging after 80 min are shown for Ly6G-Cre $JAK2^{+/+}$ (upper panels) and $JAK2^{+V/F}$ (lower panels) are shown. Left: Image projection of tree z-planes spanning 15 μm . Scale bar, 50 μm . Middle: XYZ sections of an example neutrophil on the vessel wall. Right: Neutrophil motion tracks of 120 s of imaging each. **(C-H)** Measurements of in vivo two-photon microscopy showing accumulated distance, displacement, mean velocity, directness index, and mean sphericity of 2,339 tdTomato⁺ neutrophils from Ly6G-Cre $JAK2^{+/+}$ and 2,334 tdTomato⁺ neutrophils from Ly6G-Cre $JAK2^{+V/F}$ mice ($n=3$ per condition) as well as the mean velocity of sphericity^{high} neutrophils. Neutrophils isolated exhibited the following migration parameters ($JAK2^{+/+}$ compared to $JAK2^{+V/F}$): accumulated distance of 99.7 μm compared to 79.4 μm , displacement of 10.8 μm compared to 10.0 μm , mean velocity of 0.464 $\mu\text{m}/\text{sec}$ compared to 0.365 $\mu\text{m}/\text{sec}$, and directness index of 0.12 compared to 0.15. Data are shown as mean \pm SEM. *** $p \leq 0.001$, **** $p \leq 0.0001$ (unpaired, two-tailed t-test)

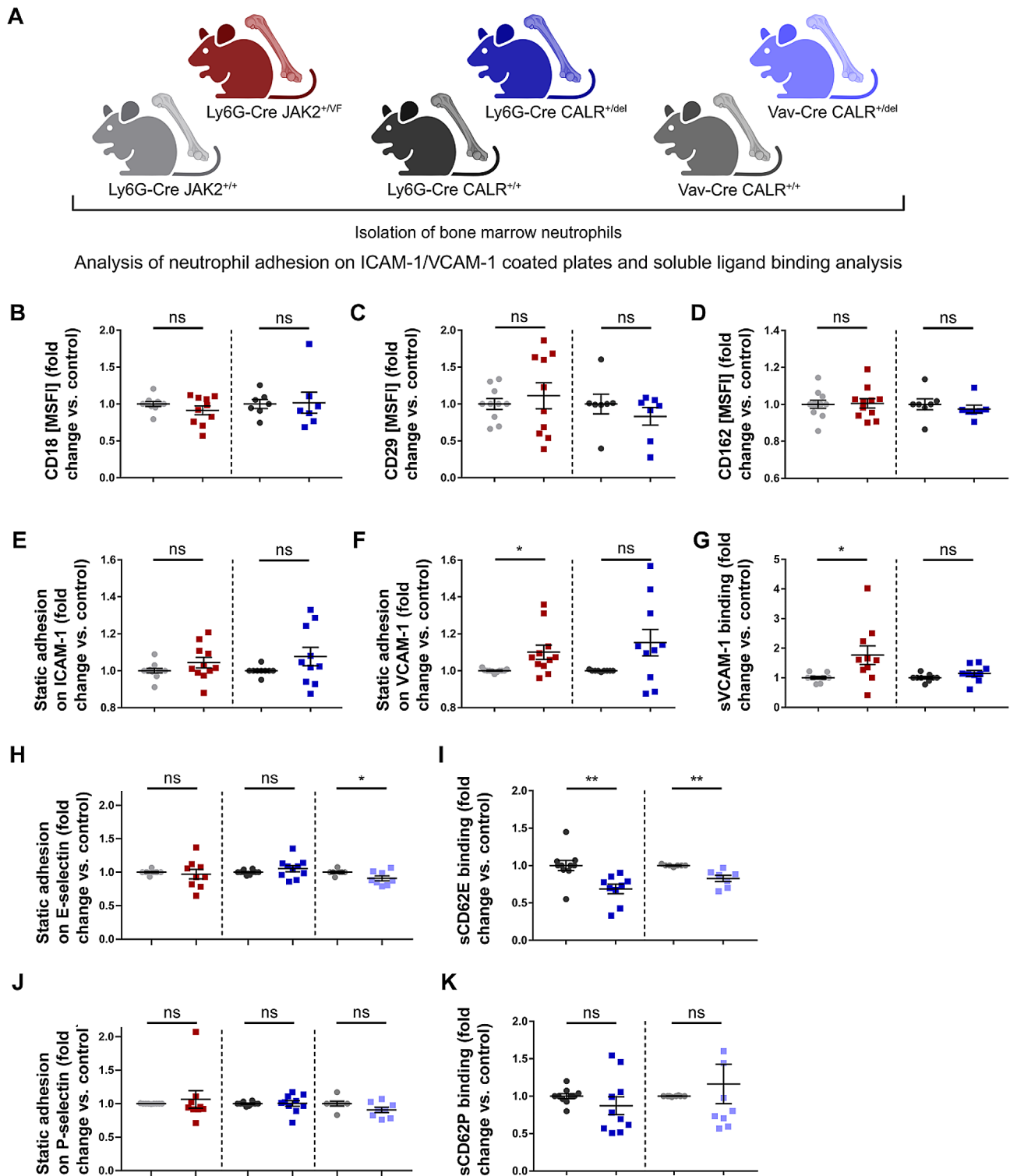


Fig. 8 (See legend on next page.)

was a considerable variability with similar patterns for both groups. Nevertheless, differences in adhesion to VCAM-1 coated surfaces between the models (Ly6G-Cre $JAK2$ -V617E, Ly6G-Cre $CALR$ del) are supported by the increase in affinity of $JAK2$ -V617E neutrophils in the

soluble soluble ligand binding assay (sVCAM-1 binding) (Fig. 8G). Here, the neutrophils of Ly6G-Cre $JAK2^{+/VF}$ mice exhibited significantly greater binding of soluble VCAM-1 (mean fold increase 1.77 ± 0.312) compared to control mice (Fig. 8G). This indicates an increased affinity

(See figure on previous page.)

Fig. 8 Adhesion and soluble ligand binding characteristic of JAK2-V617F and CALRdel-expressing neutrophils **(A)** Cartoon depicting the experimental design to study adhesion characteristics in neutrophils isolated from Ly6G-Cre $JAK2^{+/VF}$ and $CALR^{+/del}$ mice and from Vav-Cre $CALR^{+/del}$ mice in comparison to their corresponding WT controls. Created with Biorender.com. **(B-D)** Expression of CD18 ($\beta 2$ integrin), CD29 ($\beta 1$ integrin) and CD162 (PSGL-1) was evaluated as MSFI and calculated as fold change versus control. **(B, C)** Expression of CD18 ($\beta 2$ integrin) and CD29 ($\beta 1$ integrin) of tdTomato⁺ cells of Ly6G-Cre $JAK2^{+/+$ ($n = 10$), $JAK2^{+/VF}$ ($n = 10$), $CALR^{+/+}$ ($n = 7$) and $CALR^{+/del}$ mice ($n = 7$). **(D)** Expression of CD162 (PSGL-1) of tdTomato⁺ cells of Ly6G-Cre $JAK2^{+/+}$ ($n = 11$), $JAK2^{+/VF}$ ($n = 11$), $CALR^{+/+}$ ($n = 7$) and $CALR^{+/del}$ mice ($n = 7$). **(E, F)** Static adhesion of tdTomato⁺ cells isolated from $JAK2^{+/+}$ ($n = 11$), $JAK2^{+/VF}$ ($n = 11$), $CALR^{+/+}$ ($n = 9$) and $CALR^{+/del}$ mice ($n = 10$) on Fc-free ICAM-1 and VCAM-1 coated plates. Static adhesion assays revealed significant differences in tdTomato⁺ neutrophil adhesion to VCAM-1 between $JAK2^{+/+}$ and $JAK2^{+/VF}$ mice ($JAK2$ -V617F: 1.1 ± 0.038 ; WT: 1.0 ± 0.003 ; $p = 0.0163$; $n = 11$). No differences were shown in static adhesion to ICAM-1. **(G)** Soluble ligand binding to Fc-tagged VCAM-1 of tdTomato⁺ cells isolated from $JAK2^{+/+}$ ($n = 10$), $JAK2^{+/VF}$ ($n = 10$), $CALR^{+/+}$ ($n = 9$) and $CALR^{+/del}$ mice ($n = 9$). Fold change versus control analysis. Soluble ligand binding to VCAM-1/Fc was increased and significantly higher in tdTomato⁺ neutrophils of $JAK2^{+/VF}$ mice compared to their corresponding WT control (1.77 ± 0.312 ; WT: 1.0 ± 0.044 ; $p = 0.0258$; $n = 10$). $*p \leq 0.05$ (unpaired, two-tailed t-test). **(H)** Left and middle panel: Static adhesion of sorted tdTomato⁺ neutrophils isolated from $JAK2^{+/VF}$ ($n = 9$) and $CALR^{+/del}$ ($n = 10$) mice to Fc-free E-selectin coated plates in comparison to their corresponding $JAK2^{+/+}$ ($n = 9$) and $CALR^{+/+}$ ($n = 10$) controls. Right panel: Neutrophils harvested from Vav-Cre $CALR^{+/del}$ mice ($n = 8$) showed significantly impaired adhesion to immobilized E-selectin compared to Vav-Cre $CALR^{+/+}$ ($n = 7$) mice (0.91 ± 0.036 ; WT: 1.00 ± 0.016 ; $p = 0.0443$). **(I)** Binding to soluble Fc-tagged E-selectin of granulocytes isolated from Ly6G-Cre $CALR^{+/+}$ ($n = 10$), Ly6G-Cre $CALR^{+/del}$ ($n = 9$) as well as Vav-Cre $CALR^{+/+}$ ($n = 7$) and Vav-Cre $CALR^{+/del}$ ($n = 7$) mice, respectively shown as fold change versus control analysis. Binding of tdTomato⁺ granulocytes isolated from Ly6G-Cre $CALR^{+/del}$ mice to soluble E-selectin was found significantly decreased compared to Ly6G-Cre $CALR^{+/+}$ mice (0.69 ± 0.063 ; WT: 1.00 ± 0.068 ; $p = 0.0039$). Binding to soluble Fc-tagged E-selectin (sCD62E) of bone marrow granulocytes derived from Vav-Cre $CALR^{+/del}$ mice was also found significantly reduced in comparison to corresponding WT mice (0.83 ± 0.043 ; WT: 1.00 ± 0.005 ; $p = 0.0018$). $**p \leq 0.01$ (unpaired, two-tailed t-test) Exclusion of one outlier in Ly6G-Cre $CALR^{+/del}$ and Vav-Cre $CALR^{+/del}$ mice, respectively with the Grubbs' outlier test (Ly6G-Cre $CALR^{+/del}$: $G = 2.324$, $\alpha = 0.05$; Vav-Cre $CALR^{+/del}$: $G = 2.271$, $\alpha = 0.05$). **(J)** Left and middle panel: Static adhesion of sorted tdTomato⁺ neutrophils isolated from Ly6G-Cre $JAK2^{+/+}$ ($n = 9$) and $CALR^{+/del}$ ($n = 10$) mice to Fc-free P-selectin coated plates in comparison to their corresponding $JAK2^{+/+}$ ($n = 9$) and $CALR^{+/+}$ ($n = 10$) controls. Right panel: Static adhesion of isolated granulocytes from Vav-Cre $CALR^{+/del}$ ($n = 8$) and $CALR^{+/+}$ ($n = 7$) mice to Fc-free P-selectin coated plates (0.91 ± 0.04 ; WT: 1.00 ± 0.037). **(K)** Binding to soluble P-selectin/Fc (sCD62P) of neutrophils isolated from Ly6G-Cre $CALR^{+/del}$ ($n = 10$) and Vav-Cre $CALR^{+/del}$ ($n = 8$) mice compared with Ly6G-Cre $CALR^{+/+}$ ($n = 10$) and Vav-Cre $CALR^{+/+}$ ($n = 8$) control mice, respectively. Exclusion of one outlier in Vav-Cre $CALR^{+/del}$ mice with the Grubbs' outlier test ($G = 2.367$, $\alpha = 0.05$). Data are shown as mean \pm SEM. $p \leq 0.05$, $**p \leq 0.01$ (unpaired, two-tailed t-test)

of the $\beta 1$ integrin receptor VLA-4 towards VCAM-1 on $JAK2^{+/VF}$ neutrophils. It further suggests a conformational change of VLA-4 from the closed to the intermediate or open conformation [39]. In contrast to $JAK2^{+/VF}$ neutrophils, neutrophils derived from CALRdel mice did not display significant changes in either static adhesion to VCAM-1 and ICAM-1 or in soluble ligand binding (Fig. 8, E-G). Taken together, these data demonstrate that JAK2-V617F but not CALRdel alters the integrin function of VLA-4 on neutrophils resulting in a pro-adhesive phenotype. The pro-adhesive VLA4 – VCAM-1 interaction most likely accounts for the reduced motility of JAK2-V617F positive neutrophils shown in Fig. 6 and in vessels which regularly express VCAM-1 (Fig. 7). These data are novel and intriguing given the important role of granulocytic VLA-4 - VCAM-1 binding in thrombosis and the less frequent thrombotic events observed in CALR-mutant patients.

In inflamed tissues, recruitment of granulocytes from the circulation to the endothelial layer is initiated by binding to selectins resulting in low speed rolling of granulocytes on the endothelial layer [72]. Therefore, we next examined the adhesion of neutrophils isolated from Ly6G-Cre $JAK2^{+/VF}$ and $CALR^{+/del}$ mice to E-selectin and P-selectin coated plates. For E-selectin, no differences were detected between Ly6G-Cre JAK2-V617F and Ly6G-Cre CALRdel granulocytes compared to their respective WT controls (Fig. 8H, left and middle panels). However, we performed additional experiments using granulocytes isolated from Vav-Cre $CALR^{+/del}$ mice. Here, granulocytes were exposed in vivo to signals

derived from various other CALRdel positive hematopoietic and endothelial cells. Interestingly, neutrophils isolated from Vav-Cre $CALR^{+/del}$ mice showed a small but significant decrease in static adhesion to E-selectin (Fig. 8H, right panel). These data suggest that in the Vav-Cre $CALR^{+/del}$ model, signals derived from CALRdel positive cells other than neutrophils induce a decrease in the static adhesion capacity to bind to E-selectin-coated layers. However, it appears that the cell-intrinsic CALRdel signal in neutrophils is sufficient to reduce the binding affinity to soluble E-selectin by 31% in the Ly6G CALRdel model (Fig. 8I, left panel). As this is a relatively strong change and E-selectin is considered to be the most important selectin for cell trafficking to sites of inflammation, we performed additional experiments in the Vav-Cre CALRdel model. Here, the CALRdel-induced decrease in binding affinity for soluble E-selectin was confirmed in granulocytes from Vav-Cre $CALR^{+/del}$ mice (Fig. 8I, right panel). In contrast to E-selectin, static adhesion to P-selectin-coated plates and binding affinity to soluble P-selectin were similar in neutrophils derived from the three genotypes studies (Fig. 8, J and K). However, the functional implications of the above findings need to be further evaluated in future studies. PSGL-1 is the dominant ligand for P-selectin and also binds E-selectin and as shown above (Fig. 8D) was equally expressed on neutrophils isolated from Ly6G $JAK2^{+/VF}$ and $CALR^{+/del}$ mice compared to their respective WT controls. Taken together, these data highlight for the first time that CALRdel52 down-regulates neutrophil binding to E-selectin, but does not affect binding to ICAM-1 and

VCAM-1 which are regularly expressed on endothelium. In the clinical context of MPN disease, it is tempting to hypothesize that this may translate into a reduced prothrombotic risk of CALR mutant patients in comparison to JAK2-V617F positive patients.

Discussion

Unexpectedly, neutrophil-specific expression of *JAK2-V617F* in mice revealed thrombocytosis and BM-MK hyperplasia. Interestingly, hyperplasia of BM-MKs is regularly observed in PMF, where it is a diagnostic hallmark. JAK2-V617F positive MKs have been reported to significantly contribute to the MPN phenotype by inducing erythrocytosis, thrombocytosis, splenomegaly and expansion of HSPCs [73, 74]. TPO regulates PLT counts, but TPO serum levels remained unchanged in Ly6G-Cre JAK2-V617F mice. In addition to TPO, various other cytokines including IL-1 β , IL-1 α , and IL-6 have been identified to regulate both MKs and platelets [75–77]. Our in vitro studies showed that IL-1 β indeed stimulates MK differentiation of lin⁻ hematopoietic progenitors. Thus, in context with the recent discoveries that IL-1 β plays a pivotal role in JAK2-V617F-induced thrombocytosis and MK hyperplasia [17, 18], our data suggest that upregulation of IL-1 β serum levels in Ly6G-Cre *JAK2^{+VF}* mice drives or participates in generating thrombocytosis.

The inflammatory cytokine signature observed in MPN is associated with a number of constitutive symptoms compromising patients' quality of life [78]. Specific cytokine-phenotype associations and prognostically relevant plasma cytokine signatures in PMF [79] and PV [80] have been reported. Autocrine and paracrine regulation of inflammatory cytokines produced by clonal and non-clonal hematopoietic cells as well as other cell types like endothelial cells and fibroblasts play a significant role in the inflammatory serum cytokine signature [63, 81, 82]. IL-1 β plays a pivotal role in chronic inflammation of MPNs, and its connection to JAK2-V617F/CALR mutants, is widely acknowledged. It is believed that IL-1 β levels in blood or bone marrow contribute to increased secretion of inflammatory cytokines by monocytes and macrophages [83]. A recent study by Rai et al. demonstrated that the JAK2-mutant hematopoietic cells are involved in IL-1 β production and thereby induce inflammatory environment, which then helps the JAK2-V617F clones to expand and induce the MPN disease [84]. Besides, in another study by Rai et al. [17], the authors observed the beneficial effects of anti-IL1 β antibody treatment, alone or combined with ruxolitinib, on myelofibrosis. Additionally, their investigation using an IL-1 β knock-out JAK2V617F mouse model revealed that IL-1 β knockout led to reduced levels of inflammatory cytokines, consequently decreasing megakaryopoiesis and myelofibrosis. Moreover, research by Allain-Maillet

et al. [85] aimed at understanding the impact of JAK2-V617F mutation on cytokine storms found that while 26 cytokines were overexpressed in JAK2-V617F-mutated MPN patients, only IL-1, IL-1R, and IP-10 were directly induced by JAK2-V617F [85]. In contrast to the well-established association of JAK2-V617F with inflammation and cytokine production, evidence regarding CALR mutation is less abundant. In CALR-mutated ET, the only observed increases in cytokines are IL-4, IL-9, and IL-26, which are typically produced by non-mutated T-cells.

In Ly6G-Cre *JAK2^{+VF}* mice, levels of eight cytokines in the serum were observed to be upregulated by more than 1.5-fold including IL-1 α , IL-1 β , IL-2, IL-10, IL-12p40, IL-17, M-CSF, and TNF α . Interestingly, this panel of cytokines displays a substantial overlap with the upregulated plasma cytokine levels observed in JAK2-V617F positive MF patients [79]. Elevated serum levels of IL-1 α were also observed in a small cohort of MPN patients [86] and in MPLW515L-mutant mice [87]. Thus, our data illustrate that JAK2-V617F expression in neutrophils is sufficient to induce a typical MPN pro-inflammatory cytokine profile in the serum. On the contrary, upregulation of pro-inflammatory cytokines was almost absent in serum of Ly6G-Cre *CALR^{+del}* mice. This is in line with the clinical observation of less frequent inflammatory symptoms of CALR mutated MPN patients [26]. Differential expression of TNF α protein in primary hematopoietic cell populations isolated from JAK2-V617F versus CALR mutant patients has also been described by Fisher and colleagues [88].

Employing RNA-seq in neutrophils isolated from Vav-Cre *JAK2^{+VF}* and *JAK2^{+/+}* mice, we found a higher number of up-regulated inflammatory cytokines in comparison to Ly6G-Cre *JAK2^{+VF}* mice and overall enrichment in genes linked to inflammatory response. In contrast to neutrophils obtained from the Ly6G-Cre mouse models, these granulocytes had interacted with numerous other JAK2-V617F positive hematopoietic cell populations in vivo. Importantly, on the protein level, the serum cytokine signature of Vav-Cre *JAK2^{+VF}* mice [43] also shows a higher number of significantly up-regulated inflammatory cytokines (IL-1 α , CCL2, CCL11, CXCL5, CXCL9, CXCL10 as reported previously [43]) when compared to the serum cytokine profile revealed by Ly6G-Cre *JAK2^{+VF}* mice. Along this line, RNA-seq analysis of granulocytes isolated from JAK2-V617F patients showed marked up-regulation of a number of inflammatory cytokines and GSEA revealed a highly significant enrichment of IL-1 signaling genes compared to CALR-mutated patients. Together, our findings support the concept that JAK2-V617F positive neutrophils, rather than CALR mutant neutrophils, play an important role in driving chronic inflammation in MPN through an indirect

mechanism that involves MKs, MKPs and other myeloid progenitors.

Metabolic reprogramming represents a hallmark of cancer cells. Moreover, an inflammatory cell phenotype is accompanied by altered cellular bioenergetics [45, 46]. Remarkably, both the glycolytic as well as the mitochondrial respiratory activity were significantly higher in JAK2-V617F neutrophils compared to CALRdel neutrophils. This is likely driven by autocrine and paracrine inflammatory cytokines highly expressed in Ly6G-Cre *JAK2^{+VF}* mice. Rao and colleagues, although not specifically investigating neutrophils, already reported that JAK2-V617F promotes both glycolysis and mitochondrial respiration [89]. However, a direct comparison of metabolic parameters employing JAK2-V617F and CALRdel expressing neutrophils has not been reported previously.

There are several important pathophysiological angles when studying thrombosis which is a multifactorial process [90–92]. Our study is limited to the role of neutrophils. The migration of neutrophils is a fundamental component of inflammation including thromboinflammation (for reviews see Kraus & Gruber [93] and Bhuria [37]). Although our study touched the subject of thrombosis, it was beyond the scope of our paper to investigate thrombus formation per se. Rather, we focused on inflammatory activities of neutrophils and on the pathophysiological steps which are initiated by JAK2-V617F and CALRdel granulocytes, respectively immediately prior to formation of thrombosis and thereby promote thrombosis. Although degranulation of neutrophils and NETosis would certainly be interesting to look at and has been shown to be of great importance in MPN [94, 95] we are focussed on the early inflammation-induced in vivo changes in neutrophil activity before the onset of NETosis. Therefore, we studied in vitro and in vivo integrin- and selectin-controlled cell migration of neutrophils. Migration of granulocytes involves a dynamic interplay between adhesion events controlled on one side by integrins and selectins and on the other side by cytoskeletal functions [96, 97]. Exertion of cytoskeletal forces to the extracellular matrix is realized by dynamic interactions of the cytoskeleton with the adhesion molecules [93, 98–100]. Ly6G-Cre mice offer a suitable model for studying the cell-intrinsic impact of JAK2-V617F and of CALRdel on migratory behavior, since any indirect signals derived from JAK2-V617F or CALRdel positive cell lineages other than neutrophils can be excluded. Interestingly, previous work has demonstrated that neutrophils and monocytes moving along and adhering to the endothelium provide the initiating stimulus for thrombosis development [101–103]. Hence, the observed differences in migration and adhesion between JAK2-V617F and CALRdel positive neutrophils aligns with the clinical observation that JAK2-V617F is the primary driving force

of the pro-thrombotic risk in MPN whereas mutated CALR seems to have a lesser impact [26, 27].

Finally, we discovered that CALRdel52 negatively regulates cell adhesion of neutrophils to selectins. A distinct pattern of post-translational modifications is necessary for E- and P-selectin binding to PSGL-1 and to the additional E-selectin receptor CD44 [94, 95, 104]. Interestingly, E-selectin inhibition using the E-selectin antagonist GMI-1271 resulted in reduced thrombus formation in venous thrombosis models [105, 106]. A phase I study of GMI-1271 in deep vein thrombosis patients indicated that E-selectin inhibition reduced thrombus size without elevated risk of hemorrhage [107]. Thus, reduced adhesion of CALRdel52 mutant neutrophils to E-selectin together with no change in adhesion to VCAM-1 offer novel insights into the pathophysiological mechanisms underlying the less elevated thrombotic risk in CALR mutant patients as compared to JAK2-V617F patients. In their publication, Schürch et al. [108] demonstrated myeloperoxidase deficiency in homozygous CALRdel52 mutations, which was induced by impaired folding of newly synthesized myeloperoxidase due to defective CALR-mediated ER quality control in neutrophils. Considering the central role of CALR in quality control of many glycoproteins, it is tempting to hypothesize that reduced adhesion of CALR^{+del} neutrophils to E-selectin is the result of altered post-translational modifications of the PSGL-1 receptor. This is in line with the unaltered PSGL-1 levels on neutrophils isolated from Ly6G-Cre CALR^{+del} mice (Fig. 8), which suggests CALRdel52-induced PSGL-1 dysfunction as a cause of impaired binding affinity to E-selectin, possibly driven by abnormal peptide maturation. Another interesting action of CALR mutants is their effect on calcium flux [109].

Conclusions

In summary, this study provides a comprehensive analysis of neutrophils carrying JAK2-V617F or CALR mutations. Our findings highlight alterations in inflammatory cytokine production, metabolic functions, and cell migration (summarized in cartoon depicted in Fig. 9) which have implications for the differential pathophysiology of JAK2-V617F versus CALR-mutant disease.

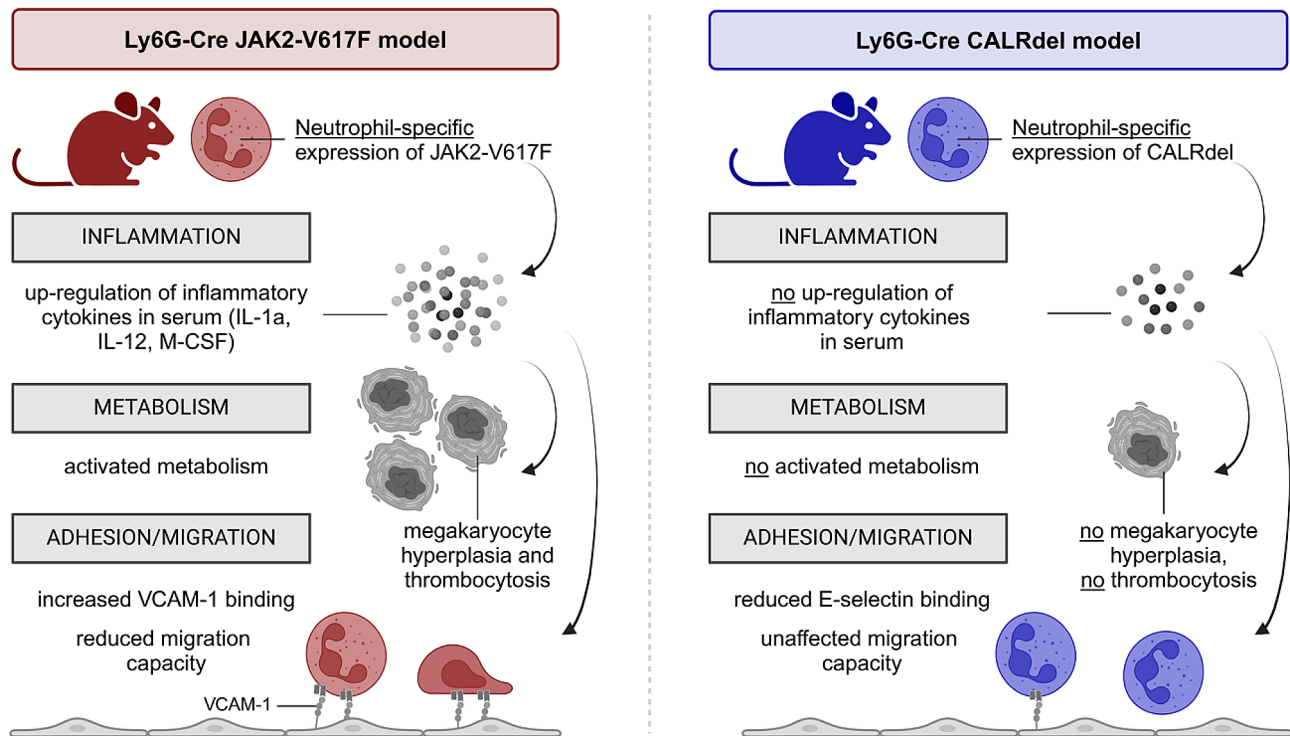


Fig. 9 Graphical summary of proposed mechanisms of action of JAK2-V617F in neutrophils. Ly6G-Cre $JAK2^{+/V617F}$ mice exhibit distinct features regarding inflammation, metabolism, adhesion, and migration compared to Ly6G-Cre $CALR^{+/del}$ mice. Created with Biorender.com

Abbreviations

MPN	Myeloproliferative neoplasms
ER	Endoplasmic reticulum
SOCE	store-operated calcium entry
TPO	Thrombopoietin
MPL	thrombopoietin receptor
CALRmut	Calreticulin mutation
JAK2	Janus kinase 2
STAT	Signal transducer and activator of transcription
PLTs	Platelets
NEUT	Neutrophil
HCT	Hematocrit
HSPCs	Hematopoietic stem and progenitor cells
MKs	Megakaryocytes
MKPs	Megakaryocyte progenitors
MEP	Megakaryocyte/erythroid progenitors
GSV	Great saphenous vein
TNF α	Tumor Necrosis Factor alpha
GM-CSF	Granulocyte-Macrophage Colony-Stimulating Factor
CXCL	C-X-C Motif Chemokine ligand
CCL	C-C Motif Chemokine ligand
CXCR	C-X-C Chemokine receptor
IL	Interleukin
IL-1 β	Interleukin-1 beta
IL-1 α	Interleukin-1 alpha

Supplementary Information

The online version contains supplementary material available at <https://doi.org/10.1186/s13045-024-01562-5>.

Supplementary Material 1

Supplementary Material 2

Supplementary Material 3

Acknowledgements

The authors thank Corinna Fahldieck and Anja Sammt for expert technical assistance and animal welfare. The authors also thank Robert Fenske (Otto-von-Guericke University, Magdeburg, Germany) for support with animal studies (Otto-von-Guericke University, Magdeburg, Germany), Priyadarshini Arunachalam (formerly Otto-von-Guericke University, Magdeburg, Germany) for performing the vena saphenous stenosis and Roland Hartig (Otto-von-Guericke University, Magdeburg, Germany) for support with FACS-based cell sorting.

Author contributions

The project was designed and supervised by T.F., T.R.H., E.C., V.B., D.M., K.F., J.D., A.D., B.S., D.B.L. and A.J.M. T.R.H., E.C., V.B., M.B., D.M., A.J.M., D.B.L. and T.F. wrote the manuscript with support of all authors. T.R.H., E.C., C.B., M.K., J.H., K.H., G.N., S.F., M.B., J.D. and A.J.M. performed experiments. J.L. and A.R.G. provided the essential CALRdel knock-in mice. All authors analyzed data, discussed and interpreted results. The authorship order among the 2 co-first authors (T.R.H. and E.C.) was assigned by giving priority to the author who initially started the project (T.R.H.).

Funding

This project was supported by research funding from Else Kröner-Forschungskolleg Magdeburg (EKFK; 2018–2021, project TP1 to TRH), from German Research Council (Deutsche Forschungsgemeinschaft (DFG); 97850925/SFB854/A20 to TF and B19 to BS), by granting a “Gerok”-position to EC and TF within the CRC854 and by 97850925/SFB854/Z01 to AD and AJM. In addition to CRC854, BS is funded by grants of the state of Saxony-Anhalt (projects SI 2 and SI 3, respectively). VB is funded by a Walter-Benjamin-Position from Deutsche Forschungsgemeinschaft (DFG) (Grant: BH 202/1–1). Open Access funding enabled and organized by Projekt DEAL.

Data availability

The datasets supporting the conclusions of this article are included within the article and its additional files. The associated Source Data can be obtained from the corresponding author upon a reasonable request.

Declarations

Ethical approval

Animal studies were approved by the government authority of Saxony-Anhalt, Germany (registration numbers: 42502-2-1496 and 42502-2-1726). Studies on human cells were approved by the local institutional review board (Ethics Committee of the Medical Faculty of Magdeburg; registration number: 61/22). Written informed consent was received prior to participation in the study.

Competing interests

D.B.L. works as a drug safety physician for Infectopharm. All other authors declare no conflict of interest.

Author details

¹Department of Hematology, Oncology, and Cell Therapy, Medical Faculty, Otto-von-Guericke University, Leipziger Str. 44, 39120 Magdeburg, Germany

²Healthcampus Immunology, Inflammation and Infectiology (GC-I, Otto-von-Guericke-University, Magdeburg, Germany

³Institute for Molecular and Clinical Immunology, Medical Faculty, Otto-von-Guericke University, Magdeburg, Germany

⁴Institute for Biochemistry and Cell Biology, Medical Faculty, Otto-von-Guericke University, Magdeburg, Germany

⁵Center for Health and Medical Prevention – CHaMP, Otto-von-Guericke University, Magdeburg, Germany

⁶Cambridge Stem Cell Institute, Department of Haematology, University of Cambridge, Cambridge, GB, England

⁷Institute for Medical Microbiology and Hospital Epidemiology, Hannover Medical School, Hannover, Germany

⁸Section of Translational Cancer Epigenomics, Division of Translational Medical Oncology, German Cancer Research Center (DKFZ), National Center for Tumor Diseases (NCT) Heidelberg, Heidelberg, Germany

⁹Faculty of Medicine, Otto-von-Guericke University, Magdeburg, Germany

¹⁰Helmholtz Centre for Infection Research, Braunschweig, Germany

Received: 22 March 2024 / Accepted: 29 May 2024

Published online: 09 June 2024

References

- Kralovics R, et al. A gain-of-function mutation of JAK2 in Myeloproliferative disorders. *N Engl J Med*. 2005;352(17):1779–90.
- Levine RL, et al. Activating mutation in the tyrosine kinase JAK2 in polycythemia vera, essential thrombocythemia, and myeloid metaplasia with myelofibrosis. *Cancer Cell*. 2005;7(4):387–97.
- James C, et al. A unique clonal JAK2 mutation leading to constitutive signaling causes polycythemia vera. *Nature*. 2005;434(7037):1144–8.
- Nangalia J, et al. Somatic CALR mutations in Myeloproliferative neoplasms with nonmutated JAK2. *N Engl J Med*. 2013;369(25):2391–405.
- Klampfl T, et al. Somatic mutations of Calreticulin in Myeloproliferative Neoplasms. *N Engl J Med*. 2013;369(25):2379–90.
- How J, Hobbs GS, Mullally A. Mutant calreticulin in myeloproliferative neoplasms. *Blood*. 2019;134(25):2242–8.
- Araki M, et al. Activation of the thrombopoietin receptor by mutant calreticulin in CALR-mutant myeloproliferative neoplasms. *Blood*. 2016;127(10):1307–16.
- Chachoua I, et al. Thrombopoietin receptor activation by myeloproliferative neoplasm associated calreticulin mutants. *Blood*. 2016;127(10):1325–35.
- Elf S, et al. Mutant calreticulin requires both its mutant C-terminus and the Thrombopoietin receptor for Oncogenic Transformation. *Cancer Discov*. 2016;6(4):368–81.
- Salati S, et al. Calreticulin Ins5 and Del52 mutations impair unfolded protein and oxidative stress responses in K562 cells expressing CALR mutants. *Sci Rep*. 2019;9(1):10558.
- Ibarra J, et al. Type I but not type II calreticulin mutations activate the IRE1 α /XBP1 pathway of the unfolded protein response to Drive Myeloproliferative Neoplasms. *Blood Cancer Discov*. 2022;3(4):298–315.
- Lau WWY, et al. The JAK-STAT signaling pathway is differentially activated in CALR-positive compared with JAK2V617F-positive ET patients. *Blood*. 2015;125(10):1679–81.
- Di Buduo CA, et al. Defective interaction of mutant calreticulin and SOCE in megakaryocytes from patients with myeloproliferative neoplasms. *Blood*. 2020;135(2):133–44.
- Pronier E, et al. Targeting the CALR interactome in myeloproliferative neoplasms. *JCI Insight*. 2018;3(22):e122703.
- Vainchenker W, Kralovics R. Genetic basis and molecular pathophysiology of classical myeloproliferative neoplasms. *Blood*. 2017;129(6):667–79.
- Grinfeld J, et al. Classification and personalized prognosis in Myeloproliferative Neoplasms. *N Engl J Med*. 2018;379(15):1416–30.
- Rai S, et al. Inhibition of interleukin-1 β reduces myelofibrosis and osteosclerosis in mice with JAK2-V617F driven myeloproliferative neoplasm. *Nat Commun*. 2022;13(1):5346.
- Rahman MF-U, et al. Interleukin-1 contributes to clonal expansion and progression of bone marrow fibrosis in JAK2V617F-induced myeloproliferative neoplasm. *Nat Commun*. 2022;13(1):5347.
- Masselli E, et al. Cytokine profiling in Myeloproliferative neoplasms: overview on phenotype correlation, Outcome Prediction, and role of genetic variants. *Cells*. 2020;9(9):2136.
- Hasselbalch HC. Perspectives on chronic inflammation in essential thrombocythemia, polycythemia vera, and myelofibrosis: is chronic inflammation a trigger and driver of clonal evolution and development of accelerated atherosclerosis and second cancer? *Blood*. 2012;119(14):3219–25.
- Rodríguez-Meira A, et al. Single-cell multi-omics identifies chronic inflammation as a driver of TP53-mutant leukemic evolution. *Nat Genet*. 2023;55(9):1531–41.
- Barbui T, et al. Polycythemia Vera: the natural history of 1213 patients followed for 20 years. *Ann Intern Med*. 1995;123(9):656.
- Tefferi A, et al. Survival and prognosis among 1545 patients with contemporary polycythemia vera: an international study. *Leukemia*. 2013;27(9):1874–81.
- Kroll MH, Michaelis LC, Verstovsek S. Mechanisms of thrombogenesis in polycythemia vera. *Blood Rev*. 2015;29(4):215–21.
- Pei YQ, et al. Prognostic value of CALR vs. JAK2V617F mutations on splenomegaly, leukemic transformation, thrombosis, and overall survival in patients with primary fibrosis: a meta-analysis. *Ann Hematol*. 2016;95(9):1391–8.
- Palova M, et al. Effect of CALR and JAK2 mutations on the clinical and hematological phenotypes of the disease in patients with myelofibrosis - long-term experience from a single center. *Neoplasma*. 2018;65(2):296–303.
- Rumi E, et al. JAK2 or CALR mutation status defines subtypes of essential thrombocythemia with substantially different clinical course and outcomes. *Blood*. 2014;123(10):1544–51.
- De Grandis M, et al. JAK2V617F activates Lu/BCAM-mediated red cell adhesion in polycythemia vera through an EpoR-independent Rap1/Akt pathway. *Blood*. 2013;121(4):658–65.
- Hobbs CM, et al. JAK2V617F leads to intrinsic changes in platelet formation and reactivity in a knock-in mouse model of essential thrombocythemia. *Blood*. 2013;122(23):3787–97.
- Etheridge SL, et al. JAK2V617F-positive endothelial cells contribute to clotting abnormalities in myeloproliferative neoplasms. *Proc Natl Acad Sci*. 2014;111(6):2295–300.
- Falanga A, et al. Leukocyte-platelet interaction in patients with essential thrombocythemia and polycythemia vera. *Exp Hematol*. 2005;33(5):523–30.
- Alvarez-Larrán A, et al. Increased platelet, leukocyte, and coagulation activation in primary myelofibrosis. *Ann Hematol*. 2008;87(4):269–76.
- Gupta N, et al. JAK2-V617F activates β 1-integrin-mediated adhesion of granulocytes to vascular cell adhesion molecule 1. *Leukemia*. 2017;31(5):1223–6.
- Marković D, et al. Neutrophil Death in Myeloproliferative neoplasms: shedding more light on neutrophils as a pathogenic link to chronic inflammation. *Int J Mol Sci*. 2022;23(3):1490.
- Barbui T, et al. Perspectives on thrombosis in essential thrombocythemia and polycythemia vera: is leukocytosis a causative factor? *Blood*. 2009;114(4):759–63.
- Ferrer-Marín F, et al. Emerging role of neutrophils in the thrombosis of chronic myeloproliferative neoplasms. *Int J Mol Sci*. 2021;22(3):1143.
- Bhuria V, et al. Thromboinflammation in Myeloproliferative Neoplasms (MPN)—A puzzle still to be solved. *Int J Mol Sci*. 2022;23(6):3206.
- Hasselbalch HC, Elvers M, Schafer AI. The pathobiology of thrombosis, microvascular disease, and hemorrhage in the myeloproliferative neoplasms. *Blood*. 2021;137(16):2152–60.
- Edelmann B, et al. JAK2-V617F promotes venous thrombosis through β 1/ β 2 integrin activation. *J Clin Invest*. 2018;128(10):4359–71.

40. Mullally A, et al. Physiological Jak2V617F expression causes a Lethal Myeloproliferative Neoplasm with Differential effects on hematopoietic stem and progenitor cells. *Cancer Cell*. 2010;17(6):584–96.
41. Hasenberg A, et al. Catchup: a mouse model for imaging-based tracking and modulation of neutrophil granulocytes. *Nat Methods*. 2015;12(5):445–52.
42. Li J, et al. Mutant calreticulin knockin mice develop thrombocytosis and myelofibrosis without a stem cell self-renewal advantage. *Blood*. 2018;131(6):649–61.
43. Müller P, et al. Anti-inflammatory treatment in MPN: targeting TNFR1 and TNFR2 in JAK2-V617F-induced disease. *Blood Adv*. 2021;5(23):5349–59.
44. Mohr J, et al. The cell fate determinant Scribble is required for maintenance of hematopoietic stem cell function. *Leukemia*. 2018;32(5):1211–21.
45. Faas M, et al. IL-33-induced metabolic reprogramming controls the differentiation of alternatively activated macrophages and the resolution of inflammation. *Immunity*. 2021;54(11):2531–e25465.
46. Friščić J, et al. The complement system drives local inflammatory tissue priming by metabolic reprogramming of synovial fibroblasts. *Immunity*. 2021;54(5):1002–e102110.
47. Hasenberg M, et al. Rapid Immunomagnetic Negative Enrichment of Neutrophil Granulocytes from Murine Bone Marrow for Functional studies in Vitro and in vivo. *PLoS ONE*. 2011;6(2):e17314.
48. Okano M, et al. Vivo imaging of venous Thrombus and pulmonary embolism using Novel Murine venous thromboembolism model. *JACC Basic Transl Sci*. 2020;5(4):344–56.
49. Formaglio P, et al. Nitric oxide controls proliferation of *Leishmania* major by inhibiting the recruitment of permissive host cells. *Immunity*. 2021;54(12):2724–e273910.
50. Dudeck J, et al. Directional mast cell degranulation of tumor necrosis factor into blood vessels primes neutrophil extravasation. *Immunity*. 2021;54(3):468–e4835.
51. Lévesque J-P, et al. Role of macrophages and phagocytes in orchestrating normal and pathologic hematopoietic niches. *Exp Hematol*. 2021;100:12–e311.
52. Cossío I, Lucas D, Hidalgo A. Neutrophils as regulators of the hematopoietic niche. *Blood*. 2019;133(20):2140–8.
53. Guo BB, et al. Megakaryocytes in Myeloproliferative Neoplasms have unique somatic mutations. *Am J Pathol*. 2017;187(7):1512–22.
54. Fisher DAC, et al. Inflammatory pathophysiology as a contributor to Myeloproliferative Neoplasms. *Front Immunol*. 2021;12:683401.
55. Hoermann G, Greiner G, Valent P. Cytokine Regulation of Microenvironmental Cells in Myeloproliferative Neoplasms. *Mediators Inflamm*. 2015;2015:1–17.
56. Turner MD, et al. Cytokines and chemokines: at the crossroads of cell signalling and inflammatory disease. *Biochim Biophys Acta - Mol Cell Res*. 2014;1843(11):2563–82.
57. Tecchio C, Micheletti A, Cassatella MA. Neutrophil-derived cytokines: facts beyond expression. *Front Immunol*. 2014;5(OCT):1–7.
58. Brizzi MF, et al. Regulation of polymorphonuclear cell activation by thrombopoietin. *J Clin Invest*. 1997;99(7). <https://doi.org/10.1172/JCI119320>.
59. Terada Y, et al. Thrombopoietin stimulates ex vivo expansion of mature neutrophils in the early stages of differentiation. *Ann Hematol*. 2003;82(11):671–6.
60. Subramanian A, et al. Gene set enrichment analysis: a knowledge-based approach for interpreting genome-wide expression profiles. *Proc Natl Acad Sci U S A*. 2005;102(43):15545–50.
61. Mootha VK, et al. PGC-1 α -responsive genes involved in oxidative phosphorylation are coordinately downregulated in human diabetes. *Nat Genet*. 2003;34(3):267–73.
62. Liberzon A, et al. The Molecular signatures Database Hallmark Gene Set Collection. *Cell Syst*. 2015;1(6):417–25.
63. Kleppe M, et al. JAK–STAT pathway activation in malignant and nonmalignant cells contributes to MPN Pathogenesis and Therapeutic Response. *Cancer Discov*. 2015;5(3):316–31.
64. Ley K, et al. Getting to the site of inflammation: the leukocyte adhesion cascade updated. *Nat Rev Immunol*. 2007;7(9):678–89.
65. Guenther C. β 2-Integrins – Regulatory and Executive bridges in the Signaling Network Controlling leukocyte trafficking and Migration. *Front Immunol*. 2022;13(JAN). <https://doi.org/10.3389/fimmu.2022.809590>.
66. De Pascalis C, Etienne-Manneville S. Single and collective cell migration: the mechanics of adhesions. *Mol Biol Cell*. 2017;28(14):1833–46.
67. Nourshargh S, Alon R. Leukocyte Migration into Inflamed tissues. *Immunity*. 2014;41(5):694–707.
68. Zengel P, et al. μ -Slide Chemotaxis: a new chamber for long-term chemotaxis studies. *BMC Cell Biol*. 2011;12(1):21.
69. Neumann J, et al. Very-late-antigen-4 (VLA-4)-mediated brain invasion by neutrophils leads to interactions with microglia, increased ischemic injury and impaired behavior in experimental stroke. *Acta Neuropathol*. 2015;129(2):259–77.
70. Huttenlocher A, Ginsberg MH, Horwitz AF. Modulation of cell migration by integrin-mediated cytoskeletal linkages and ligand-binding affinity. *J Cell Biol*. 1996;134(6):1551–62.
71. Buensuceso CS, et al. The WD protein Rack1 mediates protein kinase C and integrin-dependent cell migration. *J Cell Sci*. 2001;114(9):1691–8.
72. Silva M, Videira P, Sackstein R. E-Selectin ligands in the human mononuclear Phagocyte System: implications for infection, inflammation, and Immunotherapy. *Front Immunol*. 2018;8(JAN). <https://doi.org/10.3389/fimmu.2017.01878>.
73. Zhan H, et al. JAK2V617F-mutant megakaryocytes contribute to hematopoietic stem/progenitor cell expansion in a model of murine myeloproliferation. *Leukemia*. 2016;30(12):2332–41.
74. Woods B, et al. Activation of JAK/STAT signaling in Megakaryocytes sustains myeloproliferation in vivo. *Clin Cancer Res*. 2019;25(19):5901–12.
75. Müller-Newen G, et al. Development of platelets during steady state and inflammation. *J Leukoc Biol*. 2017;101(5):1109–17.
76. Nishimura S, et al. IL-1 α induces thrombopoiesis through megakaryocyte rupture in response to acute platelet needs. *J Cell Biol*. 2015;209(3):453–66.
77. Tilburg J, Becker IC, Italiano JE. Don't you forget about me(gakaryocytes). *Blood*. 2022;139(22):3245–54.
78. Verstovsek S, et al. Safety and efficacy of INCB018424, a JAK1 and JAK2 inhibitor, in myelofibrosis. *N Engl J Med*. 2010;363(12):1117–27.
79. Tefferi A, et al. Circulating interleukin (IL)-8, IL-2R, IL-12, and IL-15 levels are independently prognostic in primary myelofibrosis: a Comprehensive Cytokine Profiling Study. *J Clin Oncol*. 2011;29(10):1356–63.
80. Vaidya R, et al. Plasma cytokines in polycythemia vera: phenotypic correlates, prognostic relevance, and comparison with myelofibrosis. *Am J Hematol*. 2012;87(11):1003–5.
81. Ozono Y, et al. Neoplastic fibrocytes play an essential role in bone marrow fibrosis in Jak2V617F-induced primary myelofibrosis mice. *Leukemia*. 2021;35(2):454–67.
82. Erba BG, et al. Endothelial-to-mesenchymal transition in bone marrow and spleen of primary myelofibrosis. *Am J Pathol*. 2017;187(8):1879–92.
83. Hermouet S. Mutations, inflammation and phenotype of myeloproliferative neoplasms. *Front Oncol*. 2023;13(May):1196817.
84. Rai S, et al. IL-1 β promotes MPN disease initiation by favoring early clonal expansion of JAK2-mutant hematopoietic stem cells. *Blood Adv*. 2024;8(5):1234–49.
85. Allain-Maillet S, et al. Anti-glucosylsphingosine Autoimmunity, JAK2V617F-Dependent Interleukin-1 β and JAK2V617F-Independent cytokines in Myeloproliferative Neoplasms. *Cancers (Basel)*. 2020;12(9):2446.
86. Slezak S, et al. Gene and microRNA analysis of neutrophils from patients with polycythemia vera and essential thrombocytosis: down-regulation of micro RNA-1 and – 133a. *J Transl Med*. 2009;7(1):39.
87. Kleppe M, et al. Dual targeting of oncogenic activation and Inflammatory Signaling increases therapeutic efficacy in Myeloproliferative Neoplasms. *Cancer Cell*. 2018;33(1):29–e437.
88. Fisher DAC, et al. Cytokine production in myelofibrosis exhibits differential responsiveness to JAK-STAT, MAP kinase, and NF κ B signaling. *Leukemia*. 2019;33(8):1978–95.
89. Rao TN, et al. JAK2-mutant hematopoietic cells display metabolic alterations that can be targeted to treat myeloproliferative neoplasms. *Blood*. 2019;134(21):1832–46.
90. Eaton N, et al. Bleeding diathesis in mice lacking JAK2 in platelets. *Blood Adv*. 2021;5(15):2969–81.
91. Matsuura S, et al. Platelet dysfunction and thrombosis in JAK2V617F-Mutated primary myelofibrotic mice. *Arterioscler Thromb Vasc Biol*. 2020;40(10):E262–72.
92. Lamrani L, et al. Hemostatic disorders in a JAK2V617F-driven mouse model of myeloproliferative neoplasm. *Blood*. 2014;124(7):1136–45.
93. Kraus RF, Gruber MA. Neutrophils—from bone marrow to First-Line Defense of the Innate Immune System. *Front Immunol*. 2021;12:767175.
94. Wolach O, et al. Increased neutrophil extracellular trap formation promotes thrombosis in myeloproliferative neoplasms. *Sci Transl Med*. 2018;10(436):172–87.
95. Guy A, et al. Platelets and neutrophils cooperate to induce increased neutrophil extracellular trap formation in JAK2V617F myeloproliferative neoplasms. *J Thromb Haemost*. 2024;22(1):172–87.

96. Hu K, et al. Differential transmission of actin motion within focal adhesions. *Sci* (80-). 2007;315(5808):111–5.
97. Swaminathan V, Waterman CM. The molecular clutch model for mechano-transduction evolves. *Nat Cell Biol*. 2016;18(5):459–61.
98. Sixt M, et al. Cell adhesion and Migration properties of β 2-Integrin negative polymorphonuclear granulocytes on defined Extracellular Matrix molecules. *J Biol Chem*. 2001;276(22):18878–87.
99. Lindbom L, Werr J. Integrin-dependent neutrophil migration in extravascular tissue. *Semin Immunol*. 2002;14(2):115–21.
100. Burns AR, Smith CW, Walker DC. Unique structural features that influence neutrophil emigration into the lung. *Physiol Rev*. 2003;83(2):309–36.
101. von Brühl ML, et al. Monocytes, neutrophils, and platelets cooperate to initiate and propagate venous thrombosis in mice in vivo. *J Exp Med*. 2012;209(4):819–35.
102. Darbousset R, et al. Tissue factor–positive neutrophils bind to injured endothelial wall and initiate thrombus formation. *Blood*. 2012;120(10):2133–43.
103. Ruf W, Ruggeri ZM. Neutrophils release brakes of coagulation. *Nat Med*. 2010;16(8):851–2.
104. Kanamori A, et al. Distinct sulfation requirements of selectins disclosed using cells that support rolling mediated by all three selectins under shear flow. L-selectin prefers carbohydrate 6-sulfation to tyrosine sulfation, whereas P-selectin does not. *J Biol Chem*. 2002;277(36):32578–86.
105. Culmer DL, et al. E-selectin inhibition with GMI-1271 decreases venous thrombosis without profoundly affecting tail vein bleeding in a mouse model. *Thromb Haemost*. 2017;117(6):1171–781.
106. Myers D, et al. A new way to treat proximal deep venous thrombosis using E-selectin inhibition. *J Vasc Surg Venous Lymphat Disord*. 2020;8(2):268–78.
107. Devata S, et al. Use of GMI-1271, an E-selectin antagonist, in healthy subjects and in 2 patients with calf vein thrombosis. *Res Pract Thromb Haemost*. 2020;4(2):193–204.
108. Schürch PM, et al. Calreticulin mutations affect its chaperone function and perturb the glycoproteome. *Cell Rep*. 2022;41(8):111689.
109. Bhuria V, et al. Activating mutations in JAK2 and CALR differentially affect intracellular calcium flux in store operated calcium entry. *Cell Commun Signal*. 2024;22(1):186.

Publisher's Note

Springer Nature remains neutral with regard to jurisdictional claims in published maps and institutional affiliations.